

# **An Evaluation of Optical Band Gap in Photovoltaic Polymers for Solar Energy Capture**

by

Gilberto Ramos Rivera

A project submitted in partial fulfillment of the requirements for the degree of

MASTER OF ENGINEERING  
in  
CHEMICAL ENGINEERING

UNIVERSITY OF PUERTO RICO  
MAYAGÜEZ CAMPUS  
2019

Approved by:

\_\_\_\_\_  
David Suleiman, Ph.D.  
President, Graduate Committee

\_\_\_\_\_  
Date

\_\_\_\_\_  
Moses Bogere, Ph.D.  
Member, Graduate Committee

\_\_\_\_\_  
Date

\_\_\_\_\_  
Nairmen Mina, Ph.D.  
Member, Graduate Committee

\_\_\_\_\_  
Date

\_\_\_\_\_  
Ricky Valentin, Ph.D.  
Representative of Graduate School

\_\_\_\_\_  
Date

\_\_\_\_\_  
Aldo Acevedo, Ph.D.  
Chair, Department of Chemical Engineering

\_\_\_\_\_  
Date

## **ABSTRACT**

Organic solar cells are a very promising technology for use in the renewable energy field. Band gap measurements on liquid phase for different polymers were studied, and the possible radiation harvest and reasoning for band gap tendencies were established. Polymers were divided into 4 groups: commercial polymers (P3HT, Polyaniline and PTFE), SIBS related polymers, EGMEM, and PEEK, PTBAM and block polymers. Polymers were analyzed by UV-Visible spectrometry and with the Tauc's method, direct and indirect band gaps were determined for them. Radiation harvest was approximated using the spectral data from ASTM AM 1.5 spectrum and a simple Matlab code. The best results were obtained for SIBS 88, PEEK and PTBAM polymers. Band gap values for these polymers are near values reported for PCBM, which may suggest a similar behavior and performance. Sulfonation, conjugation and structure of these polymers suggest them as good candidates to be acceptor materials on organic solar devices.

## RESUMEN

Las celdas solares orgánicas son una tecnología prometedora en el campo de la energía renovable. Este proyecto estudia la banda prohibida en fase líquida para diferentes polímeros, su capacidad para capturar radiación y razones para observar tendencias en estos valores. Los polímeros fueron agrupados como: polímeros comerciales (P3HT, Polyanilina y PTFE), polímeros relacionados con SIBS, EGMEM, y PEEK, PTBAM y polímeros de bloque. Fueron analizados por espectrometría ultravioleta-visible, y utilizando el método de Tauc, valores de banda directo e indirecto fueron determinados. Con esto, el espectro ASTM AM 1.5 y un código simple de MATLAB, se aproximó la captura de radiación. Los mejores resultados fueron obtenidos para SIBS 88, PEEK y PTBAM. Sus valores se encuentran cerca de valores reportados para PCBM, lo que sugiere un comportamiento y rendimiento similares. La sulfonación, conjugación y estructura de estos polímeros les sugieren como candidatos a ser materiales receptores en dispositivos solares orgánicos.

**© Gilberto Ramos Rivera 2019**

**All Rights Reserved**

*To God, the reason behind all this journey.*

*To my family: Gilberto, Enid and Debora.*

*To Katia.*

## **ACKNOWLEDGEMENTS**

Special thanks to Dr. David Suleiman for all the advice and guidance on this academic journey. To CREST project for the financial sponsorship for great part of the master's period. To Dr. Nairmen Mina for being an accessible resource for knowledge and help. To University of Puerto Rico's Chemistry Department for allowing me to use their facilities for this project.

To my immediate family: Gilberto, Enid and Debora, for all the support along these years, for never stop believing in me and reminding me that everything is impossible until it is achieved. To Katia, thank you for listening to me, even without having any idea what I was talking about, but motivating me to continue.

# TABLE OF CONTENTS

LIST OF TABLES .....	viii
LIST OF FIGURES .....	ix
GLOSSARY OF TERMS .....	xi
<b>1 INTRODUCTION .....</b>	<b>1</b>
1.1 MOTIVATION .....	1
1.2 LITERATURE REVIEW .....	2
1.3 ORGANIC PHOTOVOLTAICS (OPVs).....	5
1.4 POLYMER SOLAR CELLS .....	6
1.5 HETEROJUNCTIONS .....	8
1.6 BAND GAP ENGINEERING.....	10
1.7 PRESENT FRAMEWORK .....	12
1.8 OBJECTIVES .....	15
1.9 PROJECT STRUCTURE.....	16
<b>2 SOLAR CELLS FUNDAMENTAL THEORY .....</b>	<b>17</b>
2.1 SOLAR SPECTRUM.....	17
2.2 SOLAR CELL PARAMETERS .....	18
2.3 PV TESTING .....	21
2.3.1 VARIABLE LOAD .....	21
2.3.2 SOURCE MEASUREMENT UNIT (SMU).....	22
2.4 DEVICE STRUCTURE.....	22
2.5 ACTIVE LAYER MATERIALS .....	24
2.5.1 INORGANIC MATERIALS.....	25
2.5.2 ORGANIC MATERIALS.....	26
2.6 BAND GAP.....	29
2.7 BAND GAP DEPENDENCE IN ORGANIC MATERIALS .....	31
2.8 DIRECT AND INDIRECT BAND GAP .....	33
2.9 BAND GAP INFLUENCE IN OPV DEVICES .....	35
<b>3 METHODOLOGY .....</b>	<b>40</b>
3.1 MATERIALS.....	40
3.2 SAMPLE PREPARATION.....	42
3.3 UV-VIS ANALYSIS.....	43
3.4 RADIATION ABSORPTION AND PHOTON FLUX HARVESTING ESTIMATION.....	45
<b>4 RESULTS &amp; DISCUSSION.....</b>	<b>47</b>
4.1 AM 1.5 SOLAR SPECTRUM CALCULATIONS .....	47
4.2 P3HT, POLYANILINE AND PTFT .....	48
4.3 SIBS AND SEBS 81.4 .....	52
4.4 PEEK, PTBAM AND BLOCK POLYMERS .....	57
4.5 PEGMEM POLYMERS.....	62
<b>5 CONCLUSION &amp; RECOMMENDATIONS .....</b>	<b>66</b>
<b>6 REFERENCES .....</b>	<b>68</b>
<b>7 APPENDIX.....</b>	<b>77</b>

## LIST OF TABLES

Table 3-1: Commercial used polymers information. ....	40
Table 3-2: Lab made polymers identification. ....	41
Table 3-3: Solvents identification list. ....	42
Table 3-4: Analyzed polymers solutions data. ....	43
Table 4-1: Band gap values from Tauc plot for P3HT, Polyaniline and PTFE. ....	50
Table 4-2: Radiation and photon flux possible achievable percentages for P3HT, Polyaniline and PTFE. ....	51
Table 4-3: SIBS 0 band gap estimation values and comparison with estimation using Anani et al. relation. ....	53
Table 4-4: Band gap results for SIBS and SEBS 81.4 runs. ....	56
Table 4-5: Radiation and photon flux harvest percent for SIBS polymers and SEBS 81.4. .....	57
Table 4-6: Radiation and photon flux estimated harvest percent for PEEK and PTBAM. .....	59
Table 4-7: Estimated radiation and photon flux harvest for PEEK, PTBAM and PEEM- PTBAM-PS co polymers. ....	61
Table 4-8: Calculated band gap values for PEGMEM polymers. ....	64
Table 4-9: Possible radiation and photon flux harvest for PEGMEM polymers. ....	65

## LIST OF FIGURES

Figure 1.1-Thin film model of Charles Fritts' work in 1883. <sup>10</sup> .....	3
Figure 1.2-Photoelectric effect. <sup>14</sup> .....	4
Figure 1.3-1930's structure of the most efficient photovoltaic devices. <sup>18</sup> .....	5
Figure 1.4-Examples of some of the most studied conjugated polymers. Top: poly(sulphur nitride), polyacetylene and poly(3-alkyl-thiophene). Bottom: poly(p- phenylene vinylene) (PPV), poly(2-methoxy-5-(20-ethylhexyloxy)-1,4- phenylvinylene) and yano-PPV. <sup>28</sup> .....	7
Figure 1.5-Two-layer heterojunction photovoltaic cell proposed by Saiciftci et al. <sup>28</sup> .....	9
Figure 1.6-Bandgap values of various conjugated polymers. <sup>37</sup> .....	11
Figure 1.7-Efficiency progress of OPVs' from 2001 to 2012. <sup>45,46</sup> .....	13
Figure 1.8-Substituents effect on bandgap for BDT unit. <sup>50</sup> .....	14
Figure 2.1-Approximated percentages of solar energy .....	17
Figure 2.2-AM0 and AM1.5 spectrums. <sup>57</sup> .....	18
Figure 2.3-IV curve example for a PV device. <sup>59</sup> .....	20
Figure 2.4-Fill Factor diagram. <sup>60</sup> .....	20
Figure 2.5-Simple PV device structure .....	23
Figure 2.6-Two stacked devices tandem solar cell layout. <sup>68</sup> .....	24
Figure 2.7-Silicon solar cell scheme of: n-type and p-type layers, depletion zone and electrons and holes movement after photon incidence. <sup>69</sup> .....	26
Figure 2.8-Photocurrent generation scheme in OPVs. Top (from left to right): exciton generation and exciton diffusion. Bottom (from right to left): exciton dissociation and charge collection. <sup>73</sup> .....	27
Figure 2.9-Comparison between inorganic and organic exciton size. <sup>75</sup> .....	28
Figure 2.10-(a) Förster energy transfer and (b) Dexter energy transfer enables diffusion of triplet excitons. The horizontal lines are HOMO and LUMO energy levels of the Donor (D) and Acceptor (A) molecule. The dashed arrows represent the simultaneous rearrangement of electronic configuration. <sup>74</sup> .....	29
Figure 2.11-Band gap difference between conductor, semiconductor and insulator. <sup>78</sup> .....	30
Figure 2.12-HOMO and LUMO energy levels for common used materials in OPVs. <sup>79</sup> ..	31
Figure 2.13-General representation of a direct band gap material (left scheme) and an indirect band gap material (right scheme). <sup>84</sup> .....	34
Figure 2.14-Bandgap and Voc relation for various organic materials. The black dashed line represents the Voc when a maximum quantum efficiency is obtained. <sup>94</sup> .....	37
Figure 2.15-Short circuit current density as function of bandgap for AM0 and AM1.5 spectrum. <sup>97</sup> .....	38
Figure 2.16-Model for P3HT bandgap effect on bulk heterojunction cell's efficiency. <sup>98</sup>	39
Figure 3.1-Chemical structure of purchased polymers. ....	40
Figure 3.2-Chemical structures of lab made analyzed polymers. ....	41
Figure 3.3-Vernier SpectroVis Plus Spectrophotometer used for UV-Vis tests. <sup>99</sup> .....	44
Figure 3.4-Matlab code for calculating the area of the AM 1.5 solar spectrum. ....	45

Figure 4.1-ASTM AM 1.5 fitted solar spectrum. ....	47
Figure 4.2-Cumulative photon flux calculated from ASTM AM1.5 solar spectrum.....	48
Figure 4.3-Band gap estimation for commercial polymers. A - P3HT direct band gap. B- P3HT indirect band gap. C- Polyaniline direct band gap. D- Polyaniline indirect band gap. E- PTFE direct band gap. F- PTFE indirect band gap.....	49
Figure 4.4-A) Direct band gap estimation for SIBS 0. B) Indirect band gap estimation for SIBS 0. ....	53
Figure 4.5-A-B: Direct and indirect band gap for SIBS 1.1. C-D: Direct and indirect band gap for SIBS 88 1% graphene oxide. F-E: Direct and indirect band gap for SIBS 88 3% graphene oxide.....	54
Figure 4.6-SEBS 81.4 direct and indirect band gap (A and B respectively). ....	56
Figure 4.7-PEEK direct and indirect band gap (A-B). PTBAM direct and indirect band gap (C-D). ....	58
Figure 4.8-Direct and indirect band gap for: PEEM60-b-PTBAM15-b-PEEM60 (A-B), PS15-b-PEEM60-b-PTBAM25-b-PEEM60-b-PS15 (C-D) and PS25-b-PEEM60-b- PTBAM15-b-PEEM60-b-PS25 (E-F).....	60
Figure 4.9-Direct and indirect band gap calculations for PEGMEM 8% block (A-B), PEGMEM 8% alternated (C-D) and PEGMEM 30% PS (E-F).....	63
Figure 7.1-Normalized absorbance for P3HT, PTFE and Polyaniline. ....	77
Figure 7.2-Normalized absorbance for SIBS and SEBS polymers.....	77
Figure 7.3-Normalized absorbance for PEEK, PTBAM and block polymers.....	78
Figure 7.4-Normalized absorbance for EGMEM polymers. ....	78

## GLOSSARY OF TERMS

AM0 – Air Mass coefficient for solar spectrum outside the Earth’s atmosphere  
AM1.5 Air Mass coefficient for solar spectrum inside the Earth’s atmosphere, used for standardized testing of solar modules and cells  
ASTM – American Society of Testing Materials  
CdS – Cadmium sulfide  
ClBz - Chlorobenzene  
CN - Cyanide  
CO<sub>2</sub> – Carbon dioxide  
Cr/Chl-a/Hg – Chromium/Chlorophyll-a/Mercury  
DTNT - bis(decyltetradecyl-thien)naphthothiadiazole]  
E<sub>g</sub> – band gap  
EGMEM – Ethylene glycol methyl ether methacrylate  
ε – dielectric constant  
FF – Fill Factor  
HOMO – Highest Occupied Molecular Orbital  
I<sub>mp</sub> – Maximum power point current  
I<sub>sc</sub> – Short circuit current  
ITO – Indium tin oxide  
IV curve – Current-Voltage curve  
LUMO – Lowest Unoccupied Molecular Orbital  
MDMO - Poly[2-methoxy-5-(3',7'-dimethyloctyloxy)  
MEH - Poly[2-methoxy-5-(2-ethylhexyloxy)  
OPVs – Organic Photovoltaics  
OSC – Organic Solar Cells  
P3HT - Poly(3-hexylthiophene-2,5-diyl)  
PBDT - Poly(benzo[1,2-*b*:4,5-*b'*]dithiophene  
PCBM - [6,6]-Phenyl C<sub>61</sub> butyric acid methyl ester  
PCE – Power Conversion Efficiency  
PEEK - Polyether ether ketone  
PEEM – Poly ether ether methacrylate  
P<sub>in</sub> – Incident power from the sun  
PITN - Poly(isothianaphthene)  
P<sub>out</sub> – Output power from the photovoltaic device  
PPV - 1,4-phenylenevinylene  
PpyV - Poly(*p*-phenylene vinylene)

PS – Polystyrene

PTB7 - Poly[[4,8-bis[(2-ethylhexyl)oxy]benzo[1,2-b:4,5-b']dithiophene-2,6-diyl][3-fluoro-2- [(2-ethylhexyl)carbonyl]thieno[3,4-b]thiophenediyl]]

PTBAM – Poly(tert-butylaminoethyl methacrylate)

PTFE - Polytetrafluoroethylene

PV - Photovoltaic

SEBS – Styrene-Ethylene-Butylene-Styrene

SIBS - Styrene—Isobutylene-Styrene

SMU – Source Measure Unit

$V_{mp}$  – Maximum power point voltage

$V_{oc}$  – Open circuit voltage

# 1 INTRODUCTION

## 1.1 Motivation

In the past few decades there have been many challenges regarding to energy production and sustainability. The global demand for energy is increasing at high rates. It is expected that by 2030, the energy demand will rise to 60% more than today.<sup>1</sup> Several times it has been stated that energy from fossil fuels represents a non-renewable source, in addition to other negative effects on the environment and health. According to that, the Intergovernmental Panel on Climate Change of the United Nations, has advised an increment in global temperatures between 1.8°C and 4°C for the end of the century, if the CO<sub>2</sub> emissions related to fossil fuel activities are not reduced.<sup>2</sup>

In the 1970's the world experienced a series of events where the global economy was affected. This energy crisis period (1967-1979) had a common denominator on the middle east countries. The most significant issue of this crisis came into play on 1973. In this year Arab oil producers imposed an embargo to the fuel to punish Occident nations for their support to Israel in their war against Egypt. This resulted in an increment of crude price from \$3 to \$12, and it led to further problems on transportation, industries, etc.<sup>3</sup> These events of the 1970's resurged the interest of many countries around the world for the renewable energy sources and their efficient development.

Throughout the years significant attention has focused on many categories such as: wind, waves and biomass. For example, wind energy production was estimated on 2004 to be 0.5% of global electricity production. The leading countries for that year were the United

States, Germany and Denmark, with a notable dominance of this last.<sup>4</sup> For the waves part, it is projected like one of the most promising technologies. One advantage that makes waves energy production attractive is its availability. When it is compared with wind energy, waves are available up to 90% of the time.<sup>5</sup>

Another alternative that took worldwide relevance was the use of solar energy to generate electricity. This option presented the opportunity to obtain energy without polluting natural resources. It offered the possibility of a clean and perdurable energy production. Solar energy will be further explored in this report.

## **1.2 Literature review**

The photovoltaic effect was discovered in 1839 by Edmond Bequerel.<sup>6</sup> This new founding consisted on the creation of voltage and electric current on a material after exposure to light. Although the photovoltaic effect was understood, no devices were fabricated on the first part of the 19<sup>th</sup> century. In 1873, Willoughby Smith discovered that selenium becomes electrically conductive when it absorbs light.<sup>7</sup> Related with this founding, W. Adams and R. Day in 1876, reported the production of electricity from light absorption without the employment of heat or moving parts.<sup>8</sup> Both, Adams and Day, attributed the generation of current on selenium due to the induced crystallization on the outer layers of the material.

The first photovoltaic cell was created on 1883 in New York. Charles Fritts coated selenium with a thin layer of gold, with the intention of letting light pass through. The coated selenium was attached to a metal plate and the thin film area was 30 cm<sup>2</sup>. The results from Fritts' experiment resulted in a power conversion efficiency (PCE) about 1% - 2%.<sup>9</sup>

A representation of selenium thin film is presented on Figure 1.1.

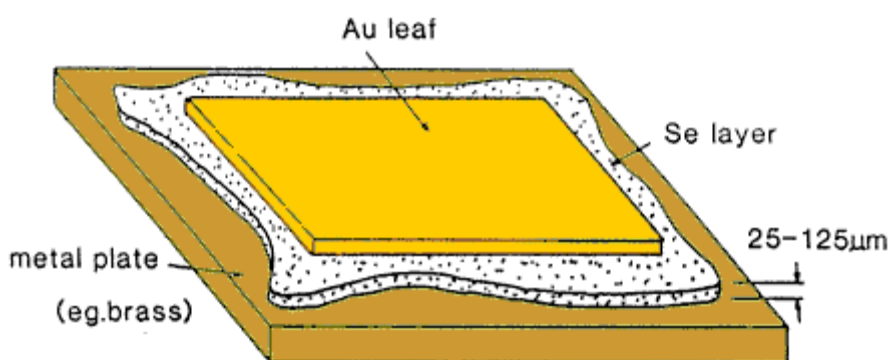


**Figure 1.1-Thin film model of Charles Fritts' work in 1883.<sup>10</sup>**

Although the 1880's represented an important historical moment, there was not a deep understanding of the photovoltaic effect at the time. For that reason, Fritts contacted a German expert ranked at the same level of Thomas Edison, Werner von Siemens. Fritts asked Siemens to replicate his experiments and confirm the findings. Siemens reported the same observations than Fritts and presented the work to the Royal Academy of Prusia.<sup>11,12</sup> On 1887, Heinrich Hertz, observed the photoelectric effect. This phenomenon consists in the expulsion of electrons from a solid surface, when it is exposed to light under the right circumstances. Hertz experiments consisted on sparks between two metal spheres on a receiver induced by the sparks generated between two metal spheres on a transmitter when they were exposed to light.<sup>13</sup> Several years after (1905), Albert Einstein presented his theory to explain the photoelectric effect, which helped him, among many other contributions to science, to receive the Nobel Prize in 1921. Figure 1.2 below is observed a simple scheme of this effect.

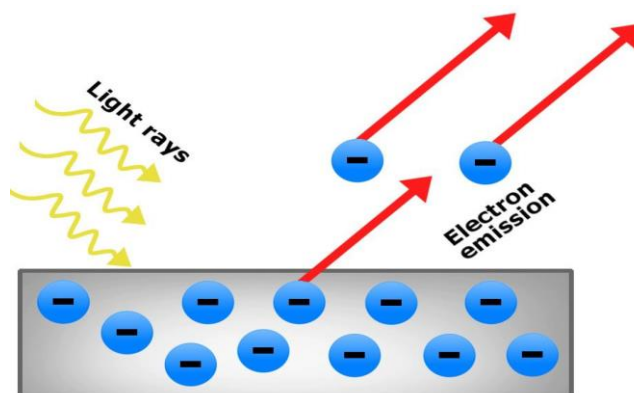


**Figure 1.2-Photoelectric effect.<sup>14</sup>**

On the first part of the 20<sup>th</sup> century organic compounds started to be considered as photoconductors. Pochettino in 1906, observed that anthracene shows conductive properties.<sup>15</sup> These observations were then confirmed by Volmer in 1913.<sup>16</sup> These works opened the door for the consideration of organic materials to produce energy from solar light.

In the 1930's, Grondahl, conducted research involving the use of copper-cuprous oxide junction. His work turned around the formation of a grid of any desired fineness. The first cells had a lead (Pb) coil inside the grid to contact it to the illuminated area on the surface.<sup>17</sup> This approach resulted to be a fructiferous area for him (38 publications). Grondahl's work reactivated the interest on selenium cells. These selenium cells were reported to be superior to the copper counterpart, and for the 1939, they became a dominant commercial product.<sup>18</sup> Figure 1.3 shown the structure of the most efficient solar cells of the 1930's.

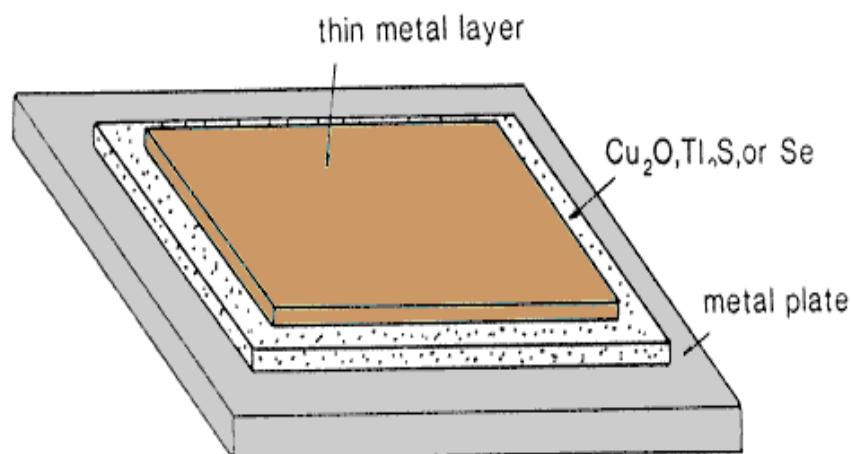


**Figure 1.3-1930's structure of the most efficient photovoltaic devices.<sup>18</sup>**

In the 1950's, Daryl Chaplin, an engineer of Bell Labs needed to develop a source of power for telephone systems in locations with high humidity. At the beginning selenium solar cells were the first approach to this purpose. The results from this were not as expected. From this failure Chaplin and two other scientist, Calvin Fuller and Gerald Pearson, discarded selenium as an option and focused on silicon. In 1954 Chaplin et al. found positive results on silicon doped with gallium.<sup>19</sup> This led to the first commercial solar cell produced in the world. Bell Labs reported it to have a PCE of 6%. In the same decade licenses for silicon photovoltaic modules began to be sold. The price was very high to saturate the market. However, spacecraft became the main field for these cells at least for the next 20 years. Today silicon photovoltaic modules encompass more than the 80% of the market.

### **1.3 Organic Photovoltaics (OPVs)**

The 1950's were excellent years for the use of organic materials for solar cells. Due to the elevated cost of silicon modules, organic materials resurged as an option. Some of the first works in this area focused on anthracene. This molecule had an advantage over others: its

crystal structure was already determined, and the availability of pure crystals was not a challenge.<sup>20</sup> Also during this period, porphyrins became one of the most studied dyes. These compounds were easy to prepare, very colored and formed crystalline films under vacuum sublimation. Other advantage porphyrins had was the fact that they could create complexes with metal ions.

During the 1960's and 70's, many works were performed on dyes. Kearns et al. (1961)<sup>21</sup>, suggested that the oxygen on the anthracene crystal surface could enhance the photoconductivity and it was demonstrated. Also Tang and Albrecht, worked with Chl-a. For this dye they found the optimal cell. It was Cr/Chl-a/Hg that had a PCE of 0.01% under monochromatic illumination.<sup>22</sup> This dye was established to be water sensitive. Ballschmitter et al. found that it was related to a adduct formation with water.<sup>23</sup> Several years of dyes research did not achieve PCEs greater than 0.1%. In 1986, Tang showed that larger efficiencies could be achieved by the production of doubled layer cells.<sup>24</sup>

#### **1.4 Polymer Solar Cells**

The second half of the 20<sup>th</sup> century represented the incubator time for the development of new approaches to the energy issues. Polymers began to be studied as optional materials for solar cells. One of the first polymers suited was poly(vinyl carbazole). This one was proposed in 1958 as an electrophotographic agent.<sup>25</sup> After that, in 1970's, other polymers captured the attention of the scientific community; poly(sulphur nitride) and polyacetylene. These two were conjugated polymers that resulted to be highly conductive when certain dopants were added. For example, in 1982 the performance of an Al/polyacetylene/graphite cell was evaluated.<sup>26</sup> The results were not positive; the efficiency achieved by the device

was only 0.3%. Four years later Glenis et al, reported the research of cells using polythiophenes.<sup>27</sup> In that case the results were similar; very low PCE. For both cases, the low efficiency was related by the author to polarons (delocalized excitons that produce an energy relaxation on the materials gap) presence. In Figure 1.4 is shown some of the most studied polymers in the 1990's.

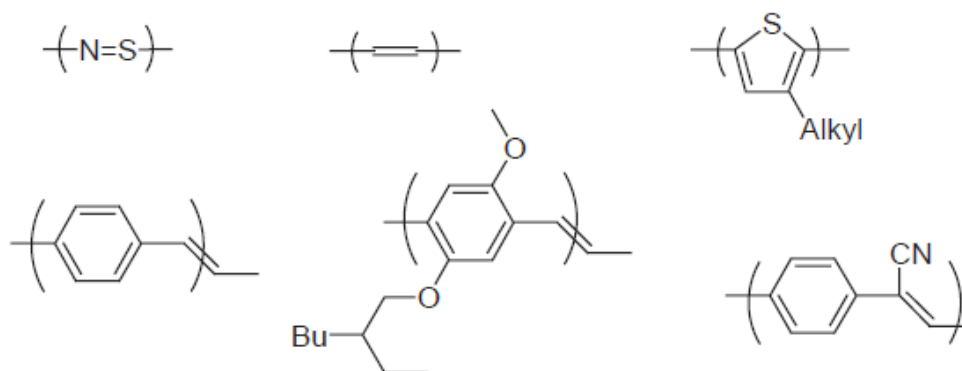


**Figure 1.4-Examples of some of the most studied conjugated polymers. Top: poly(sulphur nitride), polyacetylene and poly(3-alkyl-thiophene). Bottom: poly(p-phenylene vinylene) (PPV), poly(2-methoxy-5-(20-ethylhexyloxy)-1,4-phenylvinylene) and yano-PPV.<sup>28</sup>**

In the 1990's, poly(*p*-phenylene vinylene) (PPV) and its derivatives became the most studied polymers. Researchers were looking to find polymers with limitations on the polarons creation. Polarons are quasi-particles produced by the interaction of an electron and a surrounding deformation field. As consequence of this interaction the effective mass of the electron seems to increase, and it limits his mobility across the material. The first one that investigated PPV was Karg and his group (1993)<sup>29</sup>. They obtain a PCE of 0.1% under white light exposure. Another two researchers investigated PPV using the same structures that Karg; ITO/PPV/Al. Interestingly they obtained results very different on the cell's depletion width. Marks et al.<sup>30</sup>, had problems with their cells: they were completely depleted, while Antoniadis et al.<sup>31</sup>, found that their cells presented Schottky type barriers at the Al-interface

area. From these works the oxygen sensitivity of PPV was discovered. This behavior made an increase in the order of magnitude of the conductivity as PPV.

## 1.5 Heterojunctions

Another novel concept that started to be studied was the heterojunctions. Most of the work from diverse research groups were focused on a single layer cell using one material. Their results, as previously mentioned, were not as good as they expected. The idea of heterojunctions proposed a way to employ two materials with different electron affinities. This difference between the materials was supposed to increase the conductivity of the cells by promoting the exciton dissociation (further explained on chapter 2).

In the 1950's, researchers proved this proposal with the study of dyes on inorganic conductors. Nelson in 1956, studied the effect of having an organic dye on the surface of CdS. Their results were an increment on the conductivity of CdS in the red spectral range.<sup>32</sup> Then in the 1970's Tang, made a patent based on an idea to increase PCE beyond 0.1%. The idea was based on heterojunctions, employing a bi-layer cell made of copper and a perylene derivative. The conclusion for his work was that the heterojunction field aided in the dissociation of the excitons.

Heterojunctions presented the challenge to find at last two semiconducting materials: a donor and an acceptor. One of the most famous acceptors today known, started to be studied on the 90's: the C<sub>60</sub> fullerene. This molecule presented some advantages that made it attractive for PV cells. They were highly affine to electrons, good conductors and almost transparent. The first report on polymer/fullerene cell was made on 1993 by Sariciftci et al. The study sublimed a MEH-PPV layer that was spin coated on ITO-covered glass. The

obtained PCE for this work was 0.4%, and the current incremented in comparison with previous works, when fullerene was added.<sup>33</sup> On Figure 1.5 below is shown the Sariciftci cell structure.

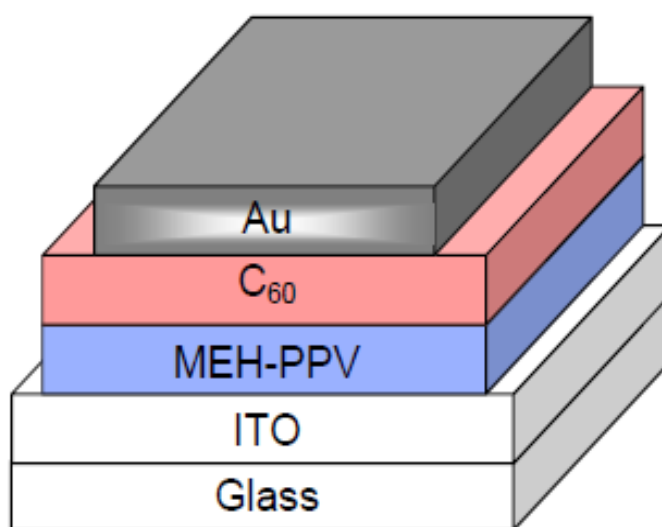


**Figure 1.5-Two-layer heterojunction photovoltaic cell proposed by Saiciftci et al.<sup>28</sup>**

From many researches on the 1990's became very clear the role of the heterojunctions on organic solar cells (OSC). Researchers learned that absorption was increased on the heterojunction, the photocurrent from the cell incremented as well. On the late stages of this decade polymer/polymer cells also became to be studied. However, they had the limitation of solubility, so the selection of pairs of polymers for research was not an easy process. In 1999 Tada et al. constructed a heterojunction solar cell that consisted of two polymers. The acceptor polymer was poly(p-pyridylvinylene) (PpyV) and the donor polymer was poly(3-hexylthiophene) (P3HT). The study concluded that photocurrent increased some three orders on magnitude when the donor polymer was present.<sup>34</sup>

Also, in these years, the first polymer/polymer bulk heterojunctions reports were published. They came, independently, from Yu et al.<sup>35</sup> and Halls et al.<sup>36</sup> in 1995. Both groups worked with CN-PPV as acceptor and MEH-PPV as the donor polymer. They studied organic layers of 100 nm thickness and found PCE of 1%. The conclusions from these works also discussed differences on the cell's performance due to morphological dependency on the polymer blend.

## **1.6 Band gap Engineering**

In addition to all the cited works, the 19<sup>th</sup> century was the cradle for a new approach in the OCS development: bandgap concerns. The bandgap of a polymer is defined as the distance difference between the valence band maximum and the conduction band minimum. This distance represents an important limitation for the electron excitation, and therefore for efficiency (more explanations on chapter 2). The efforts made on the organic photovoltaics field have followed a route of three decades and a few years. It is accepted that the first reported low band gap polymer was made by Wudl et al. on 1984.<sup>37</sup> The polymer discovered by this group was Poly(isothianaphene) (PITN). This quinoid structured polymer reported a bandgap of 1.0-1.1 eV, which represented a pioneer step on the quinoidal polymers study. However, this bandgap value was not considered a low bandgap until several years, due to the absence of bandgap categories. Was not until 1993 that Pomerantz made a rationalization of bandgap values to categorize them.<sup>38</sup> He stated that, inside a family of conjugated polymers (the most studied polymers for this moment), polyacetylene had the lowest bandgap (Figure 1.6). So, this value was the line to separate

low bandgap polymers from common bandgap ones. Those polymers with bandgap below 1.5 eV, were called low bandgap.

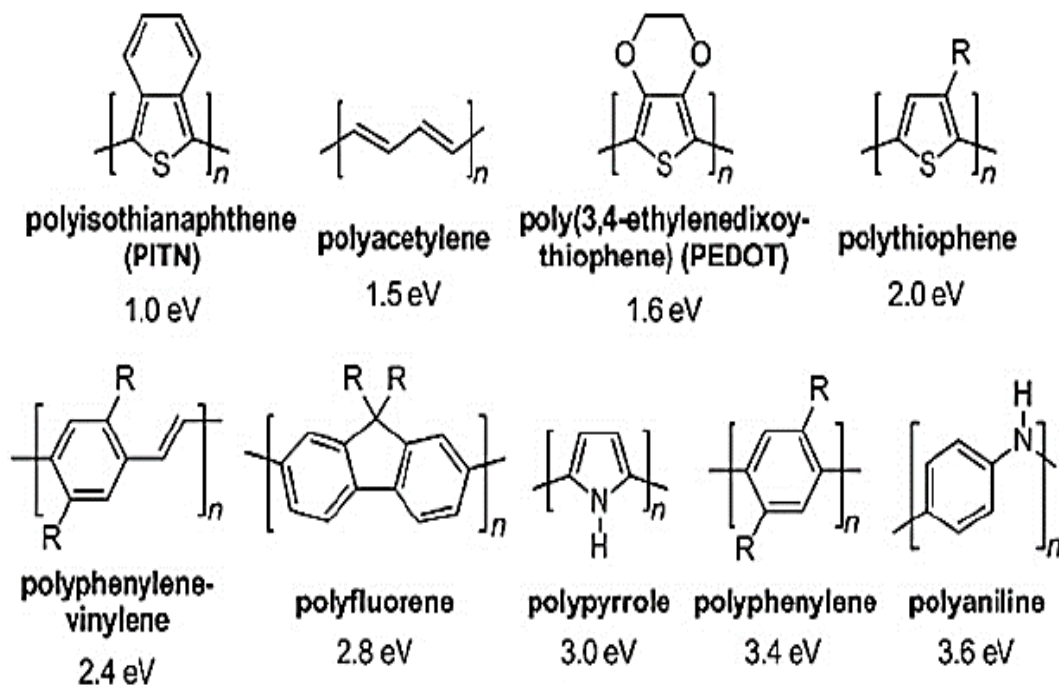


Figure 1.6-Bandgap vales of various conjugated polymers.<sup>37</sup>

During the years, many studies and efforts were focused on understanding the relationship of structure with bandgap. One of the keys proposed to lower the bandgap of some polymer were the alternation of bond length. Aromatic structures were taken as starting point. The aromatic structures show a large bandgap value, but also present the advantage of stability.<sup>39</sup> These structures represent the ground structure, so in order to reduce the bandgap, the bonds length alternation effect was theoretically studied. However, the effect of quinoidal structure to bandgap resulted to be greater than the bond length alternation. Was found that the bandgap values decrease linearly with increments of quinoidal structure to ground state.<sup>37</sup>

Another kind of study made to lower the bandgap of certain polymers was to employ fused heterocycles. As previously mentioned, PITN was the first low bandgap polymer considered. This polymer in fact, consists of a fused ring normal to the polymer backbone. In this polymer type, the main chain favors the quinoidal structure.<sup>40</sup> This has an important effect; the benzene aromaticity is maintained, and the carrier mobility possibilities are increased. In 1994, Brisset et al. achieved a 1.2 eV polymer.<sup>41</sup> The way they followed was to fuse a bithiophene with a ketal group by its  $sp^3$  carbon.

## 1.7 Present Framework

In the past decade there has been a significant development on the technology of OSC that has made it a reliable energy source. Before the beginning of the 2000's some of the fabricated devices made of polymer/ $C_{60}$  bi layers, didn't present a PCE higher than 0.1%.<sup>42</sup> The problem discussed about these devices was the poor interfacial contact area between the acceptor and donor layers. A few years later, Shoheen et al. (2003), reported OPV's made from MDMO-PPV blended with PCBM. For these cells the obtained PCE was 2.5%.<sup>43</sup> For 2007, Kim et al., reported a bulk heterojunction photovoltaic device based on 1-(3-methoxycarbonyl)propyl-1-phenyl-(6,6) $C_{61}$  within regio-regular poly(3-hexylthiophene), with PCE values exceeding the 6%.<sup>44</sup> This first decade was very productive in terms of OPV's PCE improvement. On Figure 1.7 is presented an approximated yearly development on PCE for OPV's from 2001 to 2012.

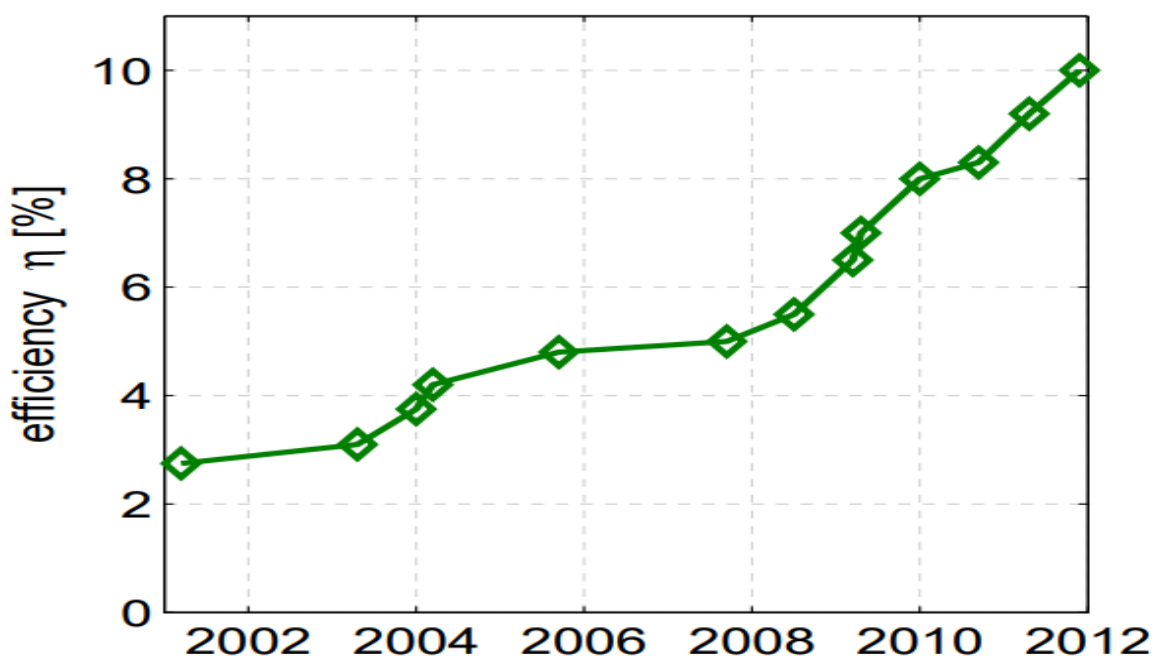


Figure 1.7-Efficiency progress of OPVs' from 2001 to 2012.<sup>45,46</sup>

In this period different materials were employed such as: quinoidal molecules, conjugated polymers, alternated donor-acceptor polymers and variations on cell's structure. Some examples of fused heterocycles researches were the works of Liang et al. in 2010. They based his work on a new benzodithiophene polymer called PTB7.<sup>47</sup> On this work, the polymer achieves a bandgap near 1.84 eV and its use on a solar cell with PC<sub>71</sub>BM resulted over 7% efficiency. Also, in 2011 Wang et al., presented the synthesis of two polymers, where the more efficient resulted to be a fusion between two benzodithiazoles with one naphthobisthiadiazole. This polymer called PBDT-DTNT, showed a bandgap of 1.93 eV, and resulted on a 6% efficiency on its respective solar cell.<sup>48</sup>

Some other approaches have also been studied with the goal of finding low bandgap polymers that improve OSC efficiency. One of the approaches used were the substitution of links in a polymer's unit to different functional groups. This bandgap tuning tool was

reported by Liang et al. in 2009. They observed a lowering on the HOMO energy of 0.1 eV, before the substitution of an alkyl side chain by an alkoxy group, on a benzodithiazole unit. In Figure 1.8 below is presented some of the substitutions made to a benzodithiazole unit and the bandgap effect.<sup>49</sup>

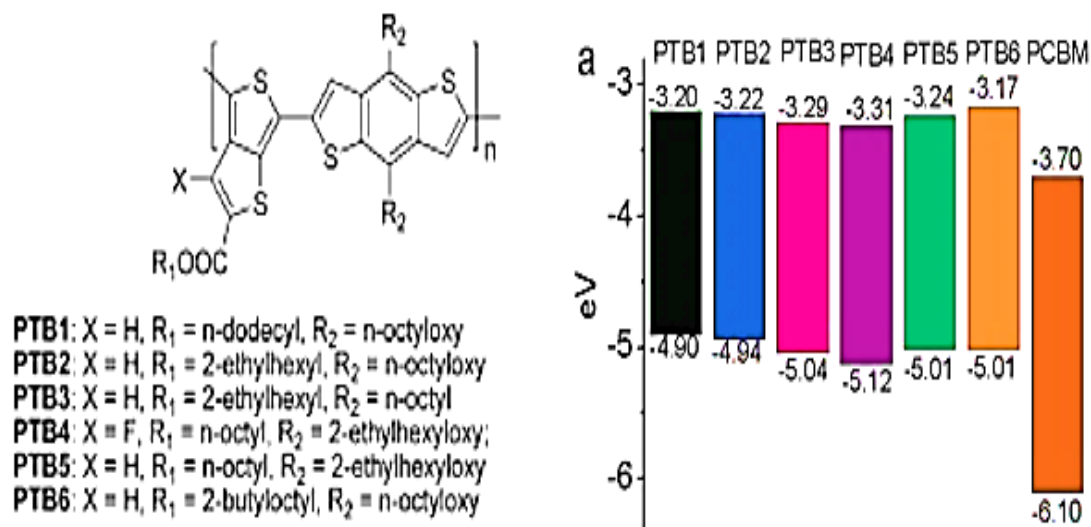


Figure 1.8-Substituents effect on bandgap for BDT unit.<sup>50</sup>

Near the unit substitution approach also appeared the donor-acceptor polymers proposal. This concept was accredited to van Mullekom et al. in 2001.<sup>51</sup> The donor-acceptor idea is to alternate rich electron structure (donors) with poor electron structure (acceptors). The first explanation about bandgap behavior related to this approach were that the alternation of electron withdrawing, and donating sections, created an inorganic analogue of a semiconductor structure named n-i-p-i. In this model, was proposed that the valence and conduction band were curved due to charge effects and this leads to a bandgap decrease. However, the most accepted explanation now considers the effect of this structure on the bond length. It proposes that the donor-acceptor alternation forms a new resonance form

of double bonding between them. When both resonance forms are averaged, this should lead to a reduced bond length alternation and therefore a lower bandgap.<sup>52,53</sup>

From 2012 the OPV field reached unthinkable efficiencies. The development of low bandgap polymers has become an important target to achieve higher PCE. The implementation of many approaches, techniques and the improvement of laboratory equipment have contributed on the OSC development field. The most recent advance in this area was reported last year, Meng et al, certified to have found a 17.3% efficiency on an inverted tandem device.<sup>54</sup> The group used two acceptor materials called 06T-4F and F-M that work better on the infrared region and therefore increment the photoconductivity of the device. With this reported value, OPV's are currently near the efficiency range of silicon cells (18%-22%).

## **1.8 Objectives**

The main objectives of this work are:

1. Discuss the importance of the bandgap concept for organic solar cells and its effect.
2. Conduct bandgap measurements for commercial and custom-made polymers in the liquid phase.
3. Discuss the reasoning behind bandgap differences among the different chemical groups of polymers.
4. Explain chemical effects or contributions to bandgap values.
5. Determine the percentage of the solar spectrum that each polymer could capture.

## **1.9 Project Structure**

This research consists of a review on theoretical basics of solar cells (inorganic and organic) in Chapter 2, methodology of the research in Chapter 3, results and discussion in Chapter 4, and the conclusion for the research is presented in Chapter 5.

## 2 SOLAR CELLS FUNDAMENTAL THEORY

### 2.1 Solar spectrum

The amount of solar energy that reaches some parts of the Earth's surface depends on many factors such as: geographical location, local landscape, weather, the time of the year, and the time of the day. Not all the radiation produced by the sun reaches the Earth. The portion that makes it, is consequently divided into two categories. The first one is the direct radiation. This type is the portion that enters the Earth's atmosphere without further obstacles; however, the amount of it is dependent of the distance that radiation must travelled through the atmosphere. The second kind is the diffuse radiation. This is the radiation diffused by the clouds and other elements present on his travel through the atmosphere. On Figure 2.1 is presented an approximation of the solar energy reflected and absorbed by the Earth's surface.

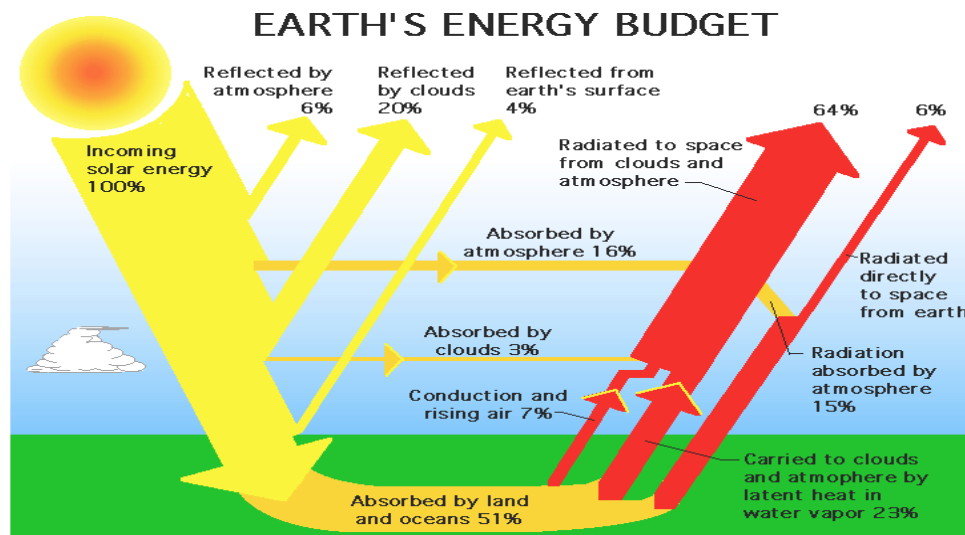


Figure 2.1-Approximated percentages of solar energy absorbed and reflected by the Earth.<sup>55</sup>

The solar spectrum outside the Earth is broad; however, the spectrum of solar energy on the Earth, is not. For that reason, the American Standard for Materials Testing (ASTM), the PV industry and the United States government, have defined two different spectrums for the solar energy.<sup>56</sup> The first one is named Air Mass 0 (AM0) and it represents the outer space spectrum. The second one is named Air Mass 1.5 (AM1.5). It describes the terrestrial radiation spectrum at standard direct normal and at a standard total spectral irradiance.

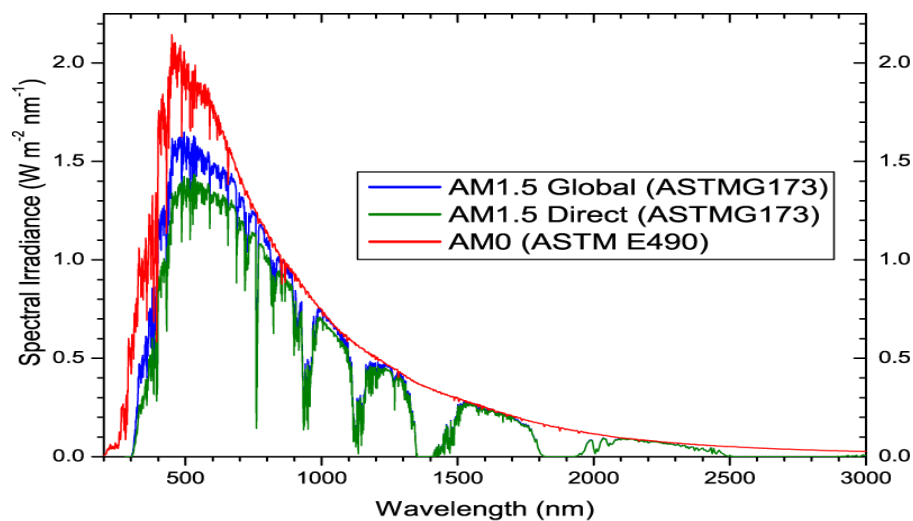


Figure 2.2-AM0 and AM1.5 spectrums.<sup>57</sup>

Figure 2.2 shows the difference between the 3 most used solar radiation spectrums. Air mass coefficient provides a relative measure of the path solar radiation must travel through the atmosphere.

## 2.2 Solar cell parameters

The objective of a PV device is the conversion of solar energy into electricity. The power conversion efficiency (PCE) (Equation 2-1) of a device is defined as the ratio between the maximum power generated ( $P_{out}$ ) and the incident power from sunlight ( $P_{in}$ ).

$$PCE = \frac{P_{out}}{P_{in}} \times 100 \quad (2-1)$$

The incident power is a function of the solar spectrum. Usually it is given in terms of AM spectrum, and is defined as (Equation 2-2):

$$AM = \frac{1}{\cos(\theta)} \quad (2-2)$$

Where  $\theta$ , corresponds to the angle of the sun when it is measured from directly overhead.

The standard value for PV device testing is  $AM=1.5$ . This value corresponds to a  $\theta=41.8^\circ$ , and a maximum power density of  $100 \frac{mW}{cm^2}$ .<sup>58</sup>

The power generated by a PV device is obtained experimentally considering the short circuit current ( $I_{sc}$ ), open circuit voltage ( $V_{oc}$ ) and the maximum power point ( $I_{mp}$ ,  $V_{mp}$ ).

The short circuit current is the maximum possible value of current that the module can deliver, and it occurs at zero voltage. It is due to the light generation and collection of carriers generated by light.  $I_{sc}$  depends on certain factors such as: solar cell area, number of photons received, incident light spectrum, optical properties of the cell and the collection probability. The open circuit voltage is the maximum voltage that can be delivered by the device (zero current). The relationship between  $I_{sc}$  and  $V_{oc}$  will be further discussed.

The maximum power point is the point at which the PV module is giving the maximum power. Usually the values for  $I_{mp}$  and  $V_{mp}$  are smaller than  $I_{sc}$  and  $V_{oc}$ , because of the non-ideality of the device. These values are obtained by realizing an IV curve for the device (Figure 2.3). The maximum power of a device is calculated by (Equation 2-3):

$$P_{out} = I_{mp} * V_{mp} \quad (2-3)$$

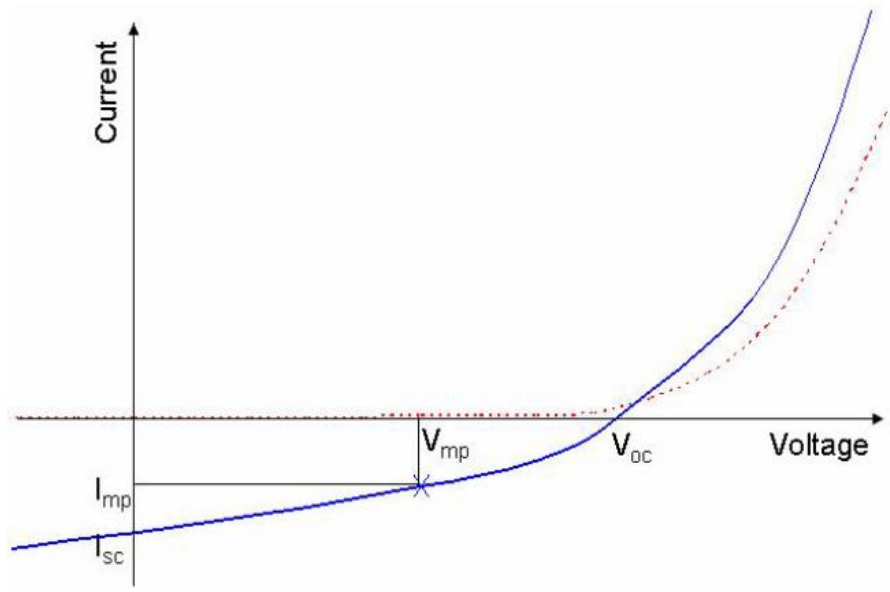


Figure 2.3-IV curve example for a PV device.<sup>59</sup>

An alternative way to find the maximum power of a device is introducing the Fill Factor (FF) parameter. A simple definition for the FF is a value of how well the maximum power rectangle created by  $I_{mp}$  and  $V_{mp}$ , fills the IV curve area. This concept is shown on Figure 2.4 below.

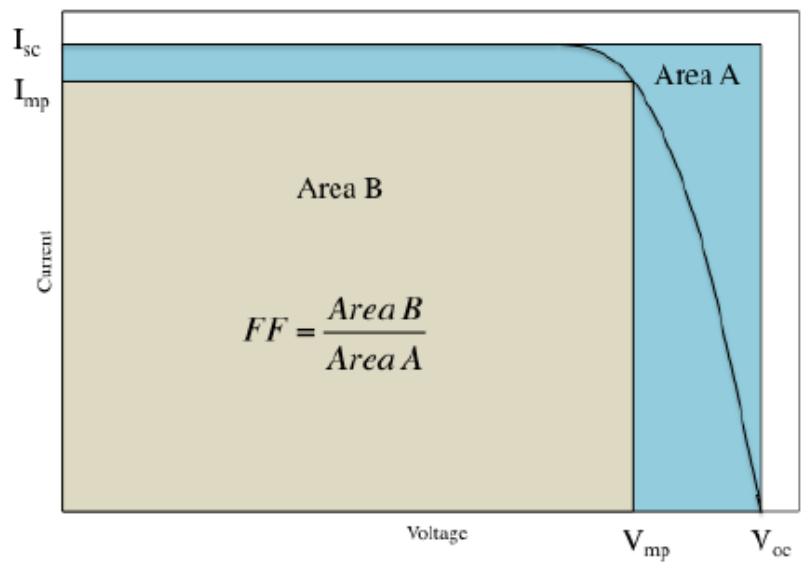


Figure 2.4-Fill Factor diagram.<sup>60</sup>

The FF is an indicative of quality for the chosen semiconductor employed on certain PV device<sup>60</sup> The equation that describes the FF is (Equation 2-4):

$$FF = \frac{I_{mp} * V_{mp}}{I_{sc} * V_{oc}} \quad (2-4)$$

With this parameter the maximum power delivered by a PV device is (Equation 2-5):

$$P_{out} = I_{sc} * V_{oc} * FF \quad (2-5)$$

## 2.3 PV testing

### 2.3.1 Variable load<sup>61</sup>

This process measures the power of a solar cell as a function of the load resistance. The steps for obtaining a current-voltage (I-V) curve is the following:

1. Measure the open circuit voltage of the illuminated cell. The load is separated from the leads and using a multimeter the voltage is measured. The current at this measurement time must be zero.
2. Measure the short circuit current on the illuminated cell. Using the multimeter, and the same set up, the current is then measured, and the voltage should be zero.
3. Attach a potentiometer in series with the solar cell and a multimeter set to current measurement. Then attach a multimeter set to voltage measurement in parallel to the potentiometer.
4. The potentiometer is then stepped through a range of resistance values. At each value, the current passing through the potentiometer and the voltage difference between each side of the potentiometer are measured.
5. The I-V curve is made by plotting the current vs voltage.

### **2.3.2 Source Measurement Unit (SMU)**

A SMU is a machine with the capacity of loading a cell with certain known current. It can measure the resulting voltage from the current addition or in the opposite order. The SMU machine steps the current load or voltage and measures the corresponding value, and this generates the I-V curve. The main limitation for this method is that the machine has a low maximum current limit. If some cell produces more current than this maximum, the I-V curve will not be accurate and reliable.

### **2.4 Device structure**

The basic structure of a PV device consists on one active material section between two metal electrodes. Figure 2.5 presents a scheme of a simple PV device. The first metal electrode must be transparent to light to allow the photons absorption on the active material. The most commonly used material for this purpose is Indium tin oxide (ITO). The materials employed for the second electrode can be varied. Some of the most commonly used are aluminum, gold, silver and lithium fluoride capped by aluminum.<sup>62, 63</sup> Independently of the chosen material for the metal electrodes, they have different work functions. This creates an electric field that helps on the movement of the excited charge carriers produced on the active material.

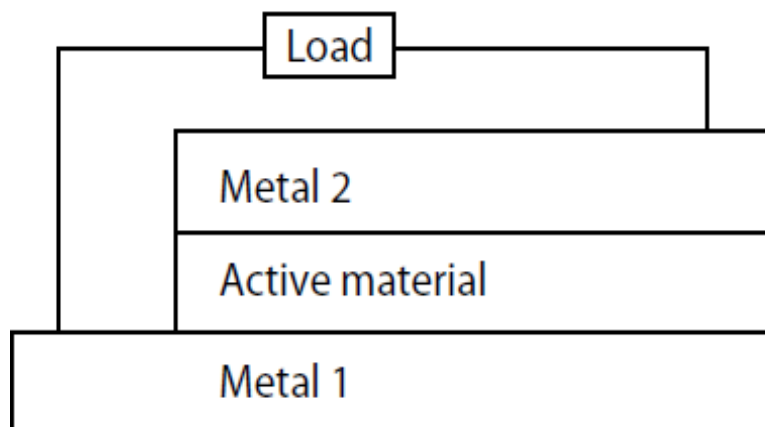


**Figure 2.5-Simple PV device structure.**

In addition to the common device structure many researches have focused on the inverted architecture. This approach looks to invert the device polarity and change the charge collection from the cell's anode to cathode. To achieve that some researchers expose the device interlayers to specific treatments in order to modify intrinsic properties of the material. As an example, Adhikary et al.<sup>64</sup>, exposed ZnO films to UV-ozone and changed the wurtzite phase crystallinity of the films. The result of their work was an improvement on the charge extraction of the films. They increase the PCE of the device from 6.46% to 8.34%.<sup>64</sup> Another approach to construct inverted solar cells is the manipulation of the electrodes work function employing surface modifier compounds. In 2012, Zhou et al., found that polymer-based compounds that contained simple aliphatic amine groups could make important reductions on the work function of many materials. Some of the materials studied were: semiconducting polymers, graphene and metal oxides.<sup>65</sup>

A third option commonly used for solar cells device architecture is the tandem structure. The tandem cells consist on the stack of two or more devices together one on top of each

other. The cells should be in contact with appropriated interlayers between them to promote the charge collection.<sup>66</sup> The main reason for the employment of this structure is the fact that semiconducting materials do not have the same absorption spectra. For that reason, the possibility to stack devices with materials having different absorption ranges helps on the improvement of the device PCE.<sup>67</sup> In Figure 2.6 presents a diagram of a tandem solar cell made of two stacked cells.

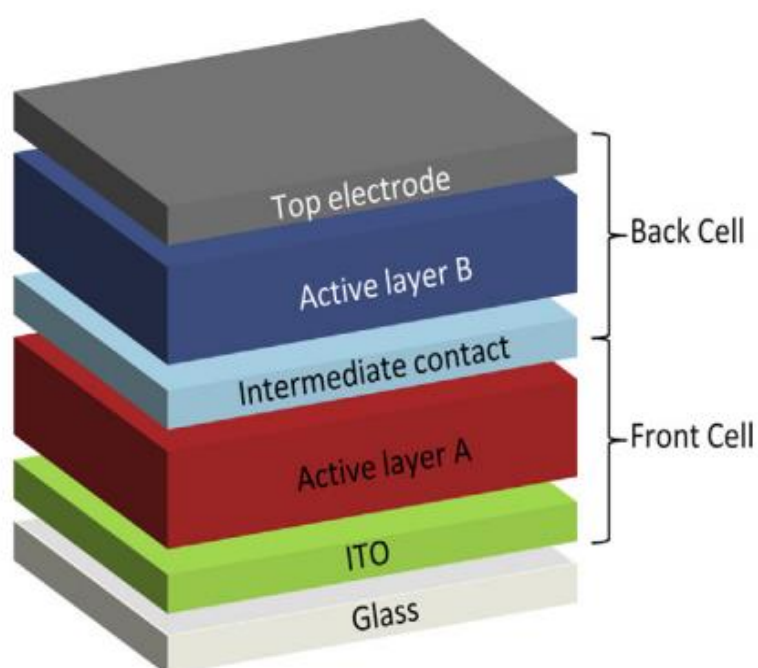


Figure 2.6-Two stacked devices tandem solar cell layout.<sup>68</sup>

## 2.5 Active layer materials

One of the most critical part of a solar cell is the active layer (AL) material. This is the cell's part where the solar light is converted into electricity for further removal and use. There is a significant difference between inorganic and organic devices in the process of sun light conversion.

### 2.5.1 Inorganic materials

Most inorganic solar cells are made of two semiconductors type: n and p. Taking one of the most common semiconductors as example, Silicon, the n-type semiconductor is made by the addition of atoms that have one more electron in their outer level in comparison to silicon. This atom makes bonds with the neighbor atoms, but one electron is left unbonded; therefore, this electron is free to move inside the silicon structure. The other case, p-type, is obtained when some atom, with one electron less than silicon in his outer level, is added to the structure. This atom as the previous case makes the bonds with the neighbor silicon atoms, but due to the electron deficiency, it creates an electron vacancy called hole.<sup>69</sup>

These two types of semiconductors are placed together in a cell, the n-type electrons jump over the p-type vacancies to fill them. The area around the junction of the two semiconductor types is called the depletion zone. When the electrons near the junction area fill the holes on their counterpart, an internal electric field is created. This field prevents electrons from the n-type layer to fill holes on the p-type layer.<sup>70</sup>

When photons strike the cell, electrons from the p-type will be ejected. The internal electric field on the cell will move the electrons to the n-type layer and, if the cell is attached with appropriated wiring, to an external circuit. At the end of the process, the electrons come back to the cell, crossing the depletion zone and going back to the external cable again. An example of the previous discussed is shown on Figure 2.7.

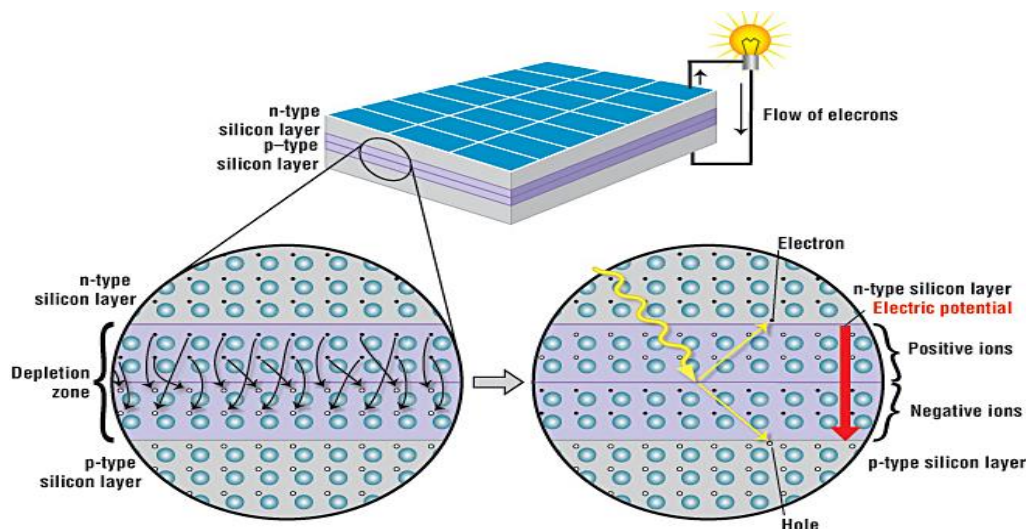


**Figure 2.7-Silicon solar cell scheme of: n-type and p-type layers, depletion zone and electrons and holes movement after photon incidence.<sup>69</sup>**

## 2.5.2 Organic materials

In contrast with the inorganic semiconductors, the photocurrent generation in OSC is a complicated process. The main difference between organic and inorganic semiconductors is the dielectric constant ( $\epsilon$ ). The dielectric constant is defined as the ratio of the electric permeability of the material to the electric permeability of free space.<sup>71</sup> Inorganic semiconductors have  $\epsilon$  values greater than 10. This value allows inorganic semiconductors to generate free electrons and holes after photons absorption. However, organic semiconductors have  $\epsilon$  values from 2-4. These dielectric constant values makes difficult the current generation across organic materials.<sup>72</sup>

The photocurrent generation of OPVs can be described in four steps: exciton generation, exciton diffusion, exciton dissociation and charge collection. Figure 2.8 shows a scheme of the process.

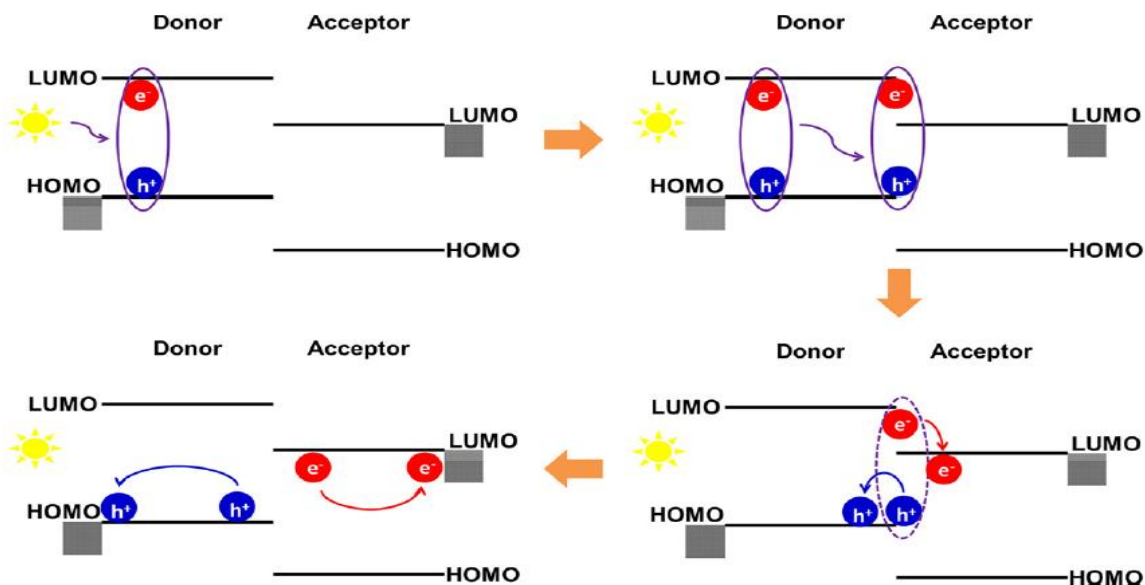


**Figure 2.8-Photocurrent generation scheme in OPVs. Top (from left to right): exciton generation and exciton diffusion. Bottom (from right to left): exciton dissociation and charge collection.<sup>73</sup>**

The first part of the process is the production of an exciton as a result of the absorption of photons. An exciton is defined as an electron-hole pair generated when a material receives a certain amount of solar energy. As an effect of low dielectric constant values, excitons produced in organic semiconductors are delocalized by 10 or more bond lengths within the organic matrix.

Excitons are neutral by nature, and because of that nature, produced excitons do not drift in electric field. Another challenge about excitons is the fact that they have a lifetime of nanoseconds and that they have a diffusion length of only of 5 nm - 20 nm.<sup>74</sup> Contrary to inorganic materials, organic excitons do not dissociate easily. In Figure 2.9 below organic and inorganic excitons are compared. The excitons from Si easily dissociate at room temperature creating a photocurrent. The organic excitons, like the  $C_{60}$  ones, hardly dissociate to free electrons and holes by thermal energy at room temperature and can easily

relax to the ground state.<sup>75</sup> For that reason, the diffusion mechanism must conduct the exciton to the donor (rich electron molecule)/acceptor (deficient electron molecule) interphase.

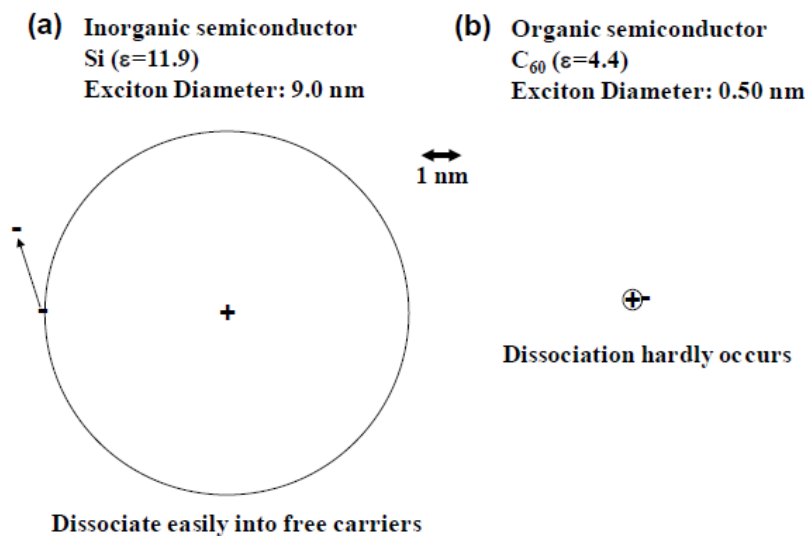


**Figure 2.9-Comparison between inorganic and organic exciton size.<sup>75</sup>**

The donor/ acceptor interphase is characterized by a great difference in electronegativity, being the acceptor the most electronegative molecule. At least two possible diffusion mechanisms have been identified as possible ways for the exciton delocalization (Figure 2.10). The first one is called the Förster mechanism. It is based on dipole-dipole interactions and occurs when the emission spectrum of the donor overlaps the absorption spectrum of the acceptor. This mechanism is through space and can be significantly observed when the donor-acceptor distance does not exceed 5 nm.<sup>76</sup> The second possible mechanism is the Dexter mechanism. This process occurs through the molecule's bonds. The transfer is performed when the donor and the acceptor are at 1 nm, so there is a part of the molecular orbitals that are significantly overlapped.<sup>77</sup>

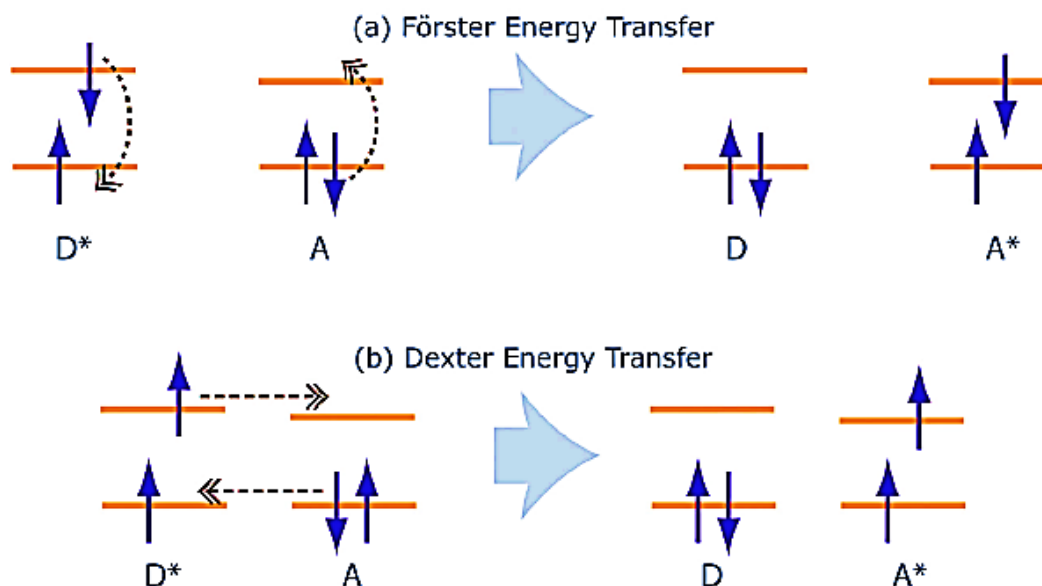


**Figure 2.10-(a) Förster energy transfer and (b) Dexter energy transfer enables diffusion of triplet excitons. The horizontal lines are HOMO and LUMO energy levels of the Donor (D) and Acceptor (A) molecule. The dashed arrows represent the simultaneous rearrangement of electronic configuration.<sup>74</sup>**

Organic excitons usually require a force larger than the exciton binding energy to dissociate it. Normally this energy is between 0.3eV-0.4eV.<sup>72</sup> Normally this separation is driven by the offset between the Lowest Unoccupied Molecular Orbital (LUMO) in donor and acceptor. Finally, the separated electrons and holes migrate to the cathode and anode respectively because of the work function of each electrode respectively. If an exciton does not reach the necessary conditions for dissociation, it will decay via radiative or non-radiative recombination.

## 2.6 Band gap

For every OPV device the bandgap ( $E_g$ ) concept is a critical parameter. This concept is defined as the distance between the valence band and the conduction band in some atom. The valence band is the outer band orbital of an atom. When electrons are excited, if they

absorb enough energy, these electrons can jump out the valence band into another band; the conduction band. This conduction band is an orbital where electrons can move freely across certain material. The band gap for some material would be then the minimum required energy to excite electrons from the valence band to the conduction band. In Figure 2.11 is presented a general scheme of the difference between conductors, semiconductors and insulators.

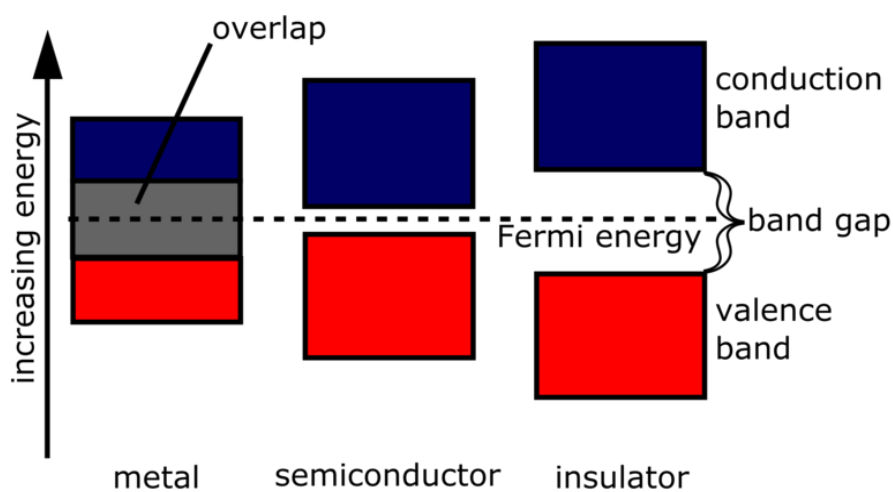


**Figure 2.11-Band gap difference between conductor, semiconductor and insulator.<sup>78</sup>**

From the Figure above is possible to note that in metals, the band gap is absent. For these materials the valence and conduction band are overlap. That is the reason why they act as electricity conductors. Insulators are materials with a greater band gap. There is a difference in the criterion used to establish an insulator bandgap value, but some authors set 9 eV as the starting point. Thus, with these limits, semiconductor materials, are the ones with band gaps near the orbitals overlap (narrow band gap semiconductors.) and near the insulators limit (wide band gap semiconductors).

## 2.7 Band gap dependence in organic materials

For organic materials,  $E_g$ , can also be defined as the energy difference between the Highest Occupied Molecular Orbital (HOMO) and the Lowest Unoccupied Molecular Orbital (LUMO). These energy values can be measured with techniques such as cyclic voltammetry. Figure 2.12 presents the HOMO and LUMO levels for some of the most commonly used donor and acceptor polymers.

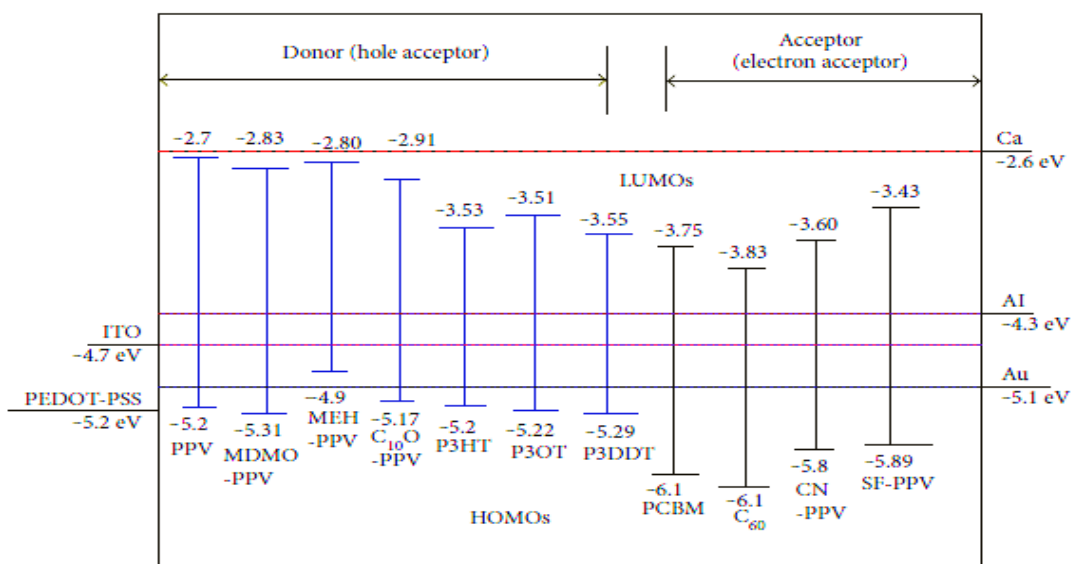


Figure 2.12-HOMO and LUMO energy levels for common used materials in OPVs.<sup>79</sup>

It has been studied that for polymeric materials, the bandgap can be modified by six parameters. These parameters are: molecular weight, bond length alternation, torsion angle, aromatic resonance energy, substituents, and intermolecular interactions.<sup>39</sup> The first parameter is the molecular weight ( $E^{Mw}$ ). In low molecular weight molecules and conjugated polymers, the HOMO and LUMO bands are constructed by the overlapping of p orbitals. This causes that the HOMO level on these molecules be filled by  $\pi$  electrons. A  $\pi$  system can undergo all electronic and optical transitions, but in counterpart the  $\sigma$  bonds

preserve the structure of the molecule by chemical bonds. Therefore for molecules or polymers, increments on the molecular weight promotes the chemical coupling of molecules and consequently the division on the HOMO and LUMO energy levels.<sup>80</sup>

$E^{\text{ör}}$  is the parameter related to the bond length difference between single and double bonds. This approach proposes that the alternation of bond lengths lowers the bandgap for organic materials. One technique recommended for OPVs materials is the alternation of donor and acceptor units across a polymer's backbone.

$E^{\theta}$  refers to the torsion angle between rings of near units. This torsion angle can be reduced by the substitution of smaller groups or the use of covalent bonds. The importance of this angle reduction is the enhancement of the polymer's planarity and this contributes to lower the bandgap.<sup>39</sup>

$E^{\text{res}}$  is the parameter linked to the aromatic resonance energy. If the aromatic unit in some polymer has a high resonance per electron the bandgap for this unit will be broader. So, the goal must be to lower the resonance of the aromatic unit until the allowed limit for chemical stability of the anti-aromatic unit.<sup>81, 82</sup>

$E^{\text{sub}}$  is related to the energy contribution that substituents make to a molecule's bandgap. Electron donating groups influence the molecule's HOMO. These groups push the electron density to the  $\pi$  system, and this push raise the corresponding energy orbitals. The resultant effect for this action is that it's easier to remove an electron from the HOMO level. However, the accepting electrons groups can also influence the molecule. These groups lower the reduction potential of the molecule and facilitate the process of pushing an electron into the LUMO. This has the effect of lowering the molecule's LUMO. In addition

to the energy contributions, substituents also help on making polymers or molecules more soluble and this facilitates its processability.

Finally,  $E^{\text{int}}$ , is the parameter related to intermolecular effects. For example, if some units interact with others, creating delocalized electrons, this interaction will lower the band gap.

In addition to the molecular parameters, temperature also plays an important role on the band gap values. The effect of temperature is described by the Varshni relation (Equation 2-6):

$$E_g = E_g(0) - \frac{\alpha T^2}{T + \beta} \quad (2-6)$$

where  $E_g(0)$ ,  $\alpha$  and  $\beta$  are fitting parameters.<sup>83</sup>

The reasoning behind this behavior is the increment of the interatomic space due to thermal effects. This interatomic spacing increment reduces the potential seen by the electrons on certain material and therefore reduces the bandgap.

## 2.8 Direct and indirect band gap

Not all semiconductors have the same electron excitation way. Two band gap types have been described for these materials: direct and indirect. The direct band gap is the easiest one to explain. In this case, the valence band maximum and the conduction band minimum, have the same  $k$  (wave vector) value. On the other hand, for indirect band gaps, the valence

band maximum and the conduction band minimum are not at the same  $k$  value (see Figure 2.13).<sup>84</sup>

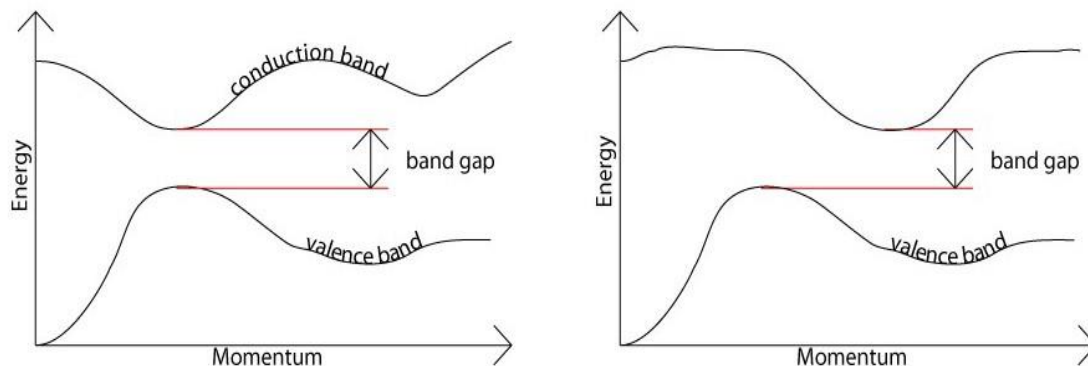


**Figure 2.13-General representation of a direct band gap material (left scheme) and an indirect band gap material (right scheme).<sup>84</sup>**

It is possible to have both band gaps on the same material. No matter that the indirect transition is the lowest energy transition of them, due to energy momentum conservation, it's difficult to this transition to result when the system is exposed to sun light. The reason for that is the fact that if a photon is absorbed, the system absorbs both the energy and the momentum of the photon. But given an energy,  $E$ , in the eV range, the momentum of the photon ( $k=E/c$ ) is extremely small, because  $c$  is so large. In consequence, the system cannot conserve momentum, while exciting an electron across an indirect band gap. All of this results in a complex process where a material with indirect band gap absorbs a photon that excites an electron, but simultaneously emits a phonon, to fulfill the energy momentum conservation. For a direct band gap material, the absorption of the photon and excitement of electrons is directly.<sup>85, 86</sup>

One of the ways to know if a material has a direct or indirect band gap is by the Tauc method. This method is often used to determine the optical band gap of semiconductors.

Basically, it starts from the relation (Equation 2-7):

$$\alpha h\nu = A(h\nu - E_g)^n \quad (2-7)$$

where  $h$  is the Planck's constant,  $\nu$  is the frequency of light, and  $E_g$  is the band gap energy.

The value of the exponent  $n$  is related to the electronic nature of the band gap, it can be 2 for indirect transitions and  $1/2$  for direct transitions.<sup>87, 88</sup> The process of the estimation of the average band gap relies on (Equation 2-8):

$$(\alpha h\nu)^{\frac{1}{n}} = A^{\frac{1}{n}} (h\nu - E_g) \quad (2-8)$$

For the direct case  $n = 1/2$ , so the Tauc plot used is  $(\alpha h\nu)^2$  vs  $h\nu$ . In the case of the indirect transition the plot is made using  $n = 2$ , so it is  $(\alpha h\nu)^{1/2}$  vs  $h\nu$ .

The band gap is estimated by the intercept of the linear part of the graph with the x axis ( $h\nu$ ).

## 2.9 Band gap influence in OPV devices

All parameters of any OPV device depend on bandgap. The  $E_g$  value for certain organic material limits the number of photons that can be absorbed by the cell. The most common example is silicon. Silicon, having a bandgap of 1.1 eV, is capable of harvesting near 77% of the solar energy.<sup>89</sup> The majority of the semiconducting polymers have bandgaps over 2 eV.<sup>90</sup> With these values, the most common scenario is a solar energy harvest of near 30% on the better cases. So, the goal is to lower the bandgap to achieve a larger amount of solar energy harvest.

However, the bandgap effects of OPVs do not only circumscribe to the photon flux harvest, it influences all the device. One of the most critical parameters for OPVs,  $V_{oc}$ , is directly affected by modifications of a material's bandgap. In the radiative recombination limit, assuming full collection of all generated carriers, and that the semiconductor structure in the ray optics limit, the  $V_{oc}$  is defined as (Equation 2-9):

$$qV_{oc} = E_g \left(1 - \frac{T}{T_{sun}}\right) - kT \ln \left(\frac{\Omega_{emit}}{\Omega_{sun}}\right) + \ln \left(\frac{4n^2}{I}\right) - \ln(QE) \quad (2-9)$$

Where:  $E_g$  = bandgap,  $T$  = solar cell temperature,  $T_{sun}$  = temperature of the sun,  $k$  = Boltzmann constant,  $\Omega_{emit}$  = solid angle of incoming photons,  $\Omega_{sun}$  = solid angle of emitted photons,  $n$  = refractive index,  $I$  = light concentration factor and  $QE$  = quantum efficiency.<sup>91</sup>

From this equation it is possible to note that the first term is like a Carnot's machine efficiency. The importance of this term is the fact that temperature will influence on the contribution of  $E_g$  to the  $V_{oc}$ , and this contribution is the largest one. According to the work of Polman and Landsberg, this first term on the  $V_{oc}$  equation could represent an energy loss up to 12%.<sup>91, 92</sup> With this is important to highlight that  $V_{oc}$  will be always below  $E_g$  due to the effect of the three other entropic terms. For almost all solar cells  $V_{oc}$  is 400-500 mV below  $E_g$ .<sup>93</sup>

From the previous presented reasons, bandgap and  $V_{oc}$  share a proportional behavior. In Figure 2.14 presents a general description of the  $E_g - V_{oc}$  relationship for various materials under AM 1.5 illumination.

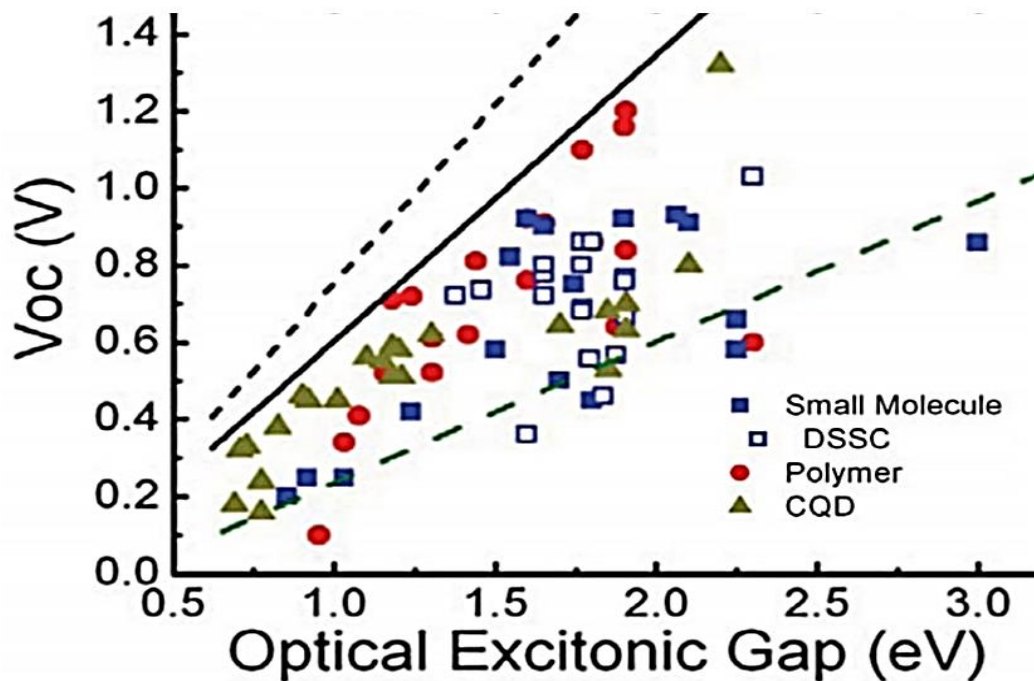
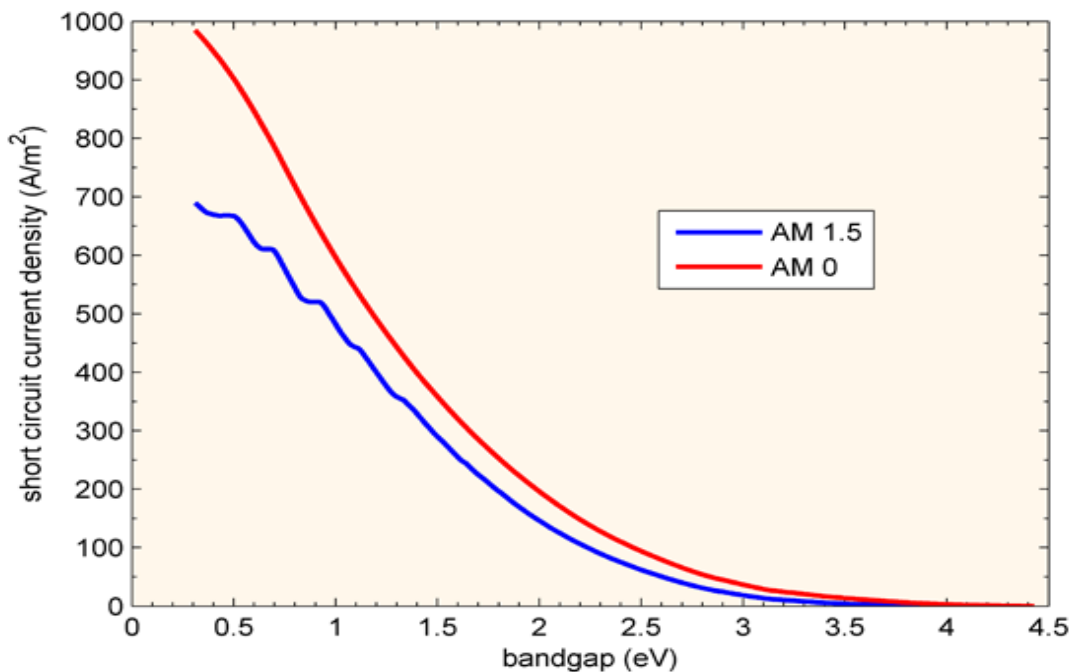


Figure 2.14-Bandgap and  $V_{oc}$  relation for various organic materials. The black dashed line represents the  $V_{oc}$  when a maximum quantum efficiency is obtained.<sup>94</sup>

However, it is important to mention that  $V_{oc}$  will increase as the recombination current falls, but there will occur a  $V_{oc}$  drop when  $I_{sc}$  is too small.<sup>95</sup>

Another important parameter that affects OPVs is the  $I_{sc}$ . The band gap of certain materials act like a stairway's step. When the photons from sun light have equal or more energy than the band gap, they make excitons and follow the previously discussed mechanism.<sup>96</sup> For this reason,  $E_g$  becomes a limiting barrier for current generation (Figure 2.15). If it is too high, a few electrons will be excited, and the photocurrent generation will be low. On the other side, when  $E_g$  is too small, many electrons will be excited, and many excitons will be available for photocurrent generation. The issue with this last case is that considering the exciton's short life and diffusion length, a high availability of excitons due to low band gap, does not mean that all excitons will end being diffused, dissociated and the charges

collected. If the excess of excited electrons cannot be handled on the donor matrix, the exciton will decay by radiative or non-radiative recombination causing  $I_{sc}$  density losses.



**Figure 2.15-Short circuit current density as function of bandgap for AM0 and AM1.5 spectrum.<sup>97</sup>**

Because of the effect that  $E_g$  has on  $V_{oc}$  and  $I_{sc}$  it is intuitive to think that the PCE is also influenced by it. In fact, it is real, the bandgap of the absorbing material is crucial on the possible PCE value for a solar cell. On Figure 2.16 is shown a predictive model for the band gap effect of P3HT on a fullerene bulk heterojunction's efficiency. It is important to note that for his case an optimum value will be around 1.9 eV. Some authors define the optimum band gap for donor materials at 1.4 eV as well.<sup>96</sup>

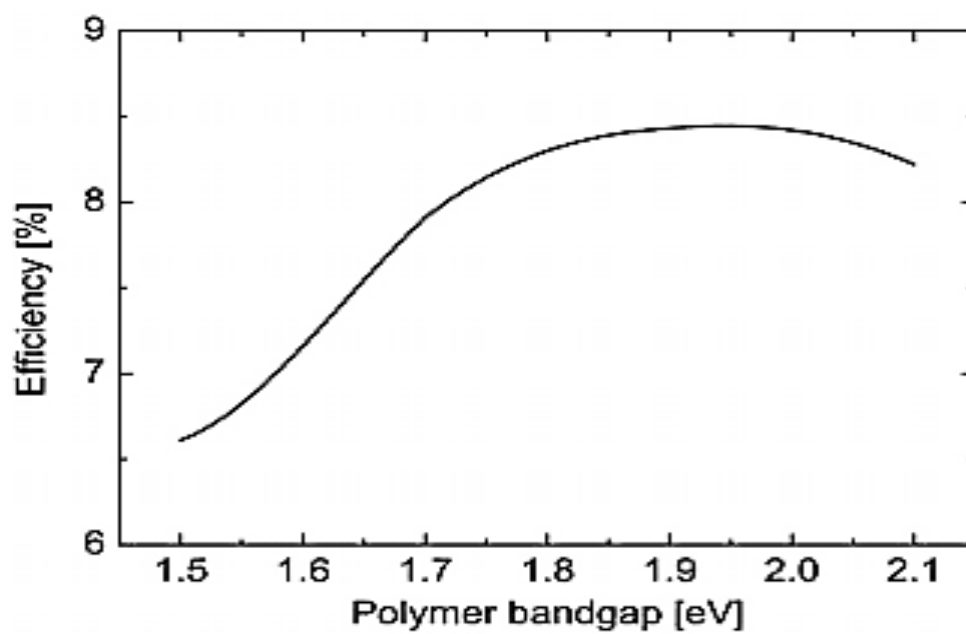


Figure 2.16-Model for P3HT bandgap effect on bulk heterojunction cell's efficiency.<sup>98</sup>

### 3 METHODOLOGY

#### 3.1 Materials

For this project two types of polymers were studied; commercial and lab made polymers. The commercial polymers specifications are listed below. Table 3-1 presents the manufacturers and important specifications and on Figure 3.1 the corresponding chemical structure of each polymer.

**Table 3-1: Commercial used polymers information.**

Polymer	Specifications	Provider
P3HT	Regio regular Mw:20,000-45,000	Sigma Aldrich
Poly(tetrafluoroethylene)	1 $\mu$ m particle size	Sigma Aldrich
Polyaniline (emeraldine salt)	Short chain, grafted to lignin	Sigma Aldrich

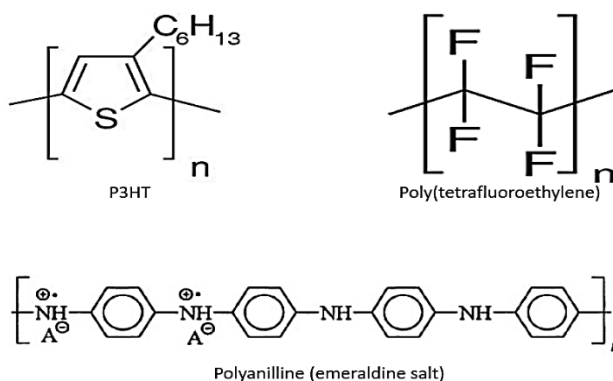


**Figure 3.1-Chemical structure of purchased polymers.**

In addition to commercial polymers, the major part of studied compounds was lab made polymers from our Polymer Nanocomposite Membrane research group. The list of the lab

made studied polymers is shown on Table 3-2 and some of their chemical structures are presented on Figure 3.2.

**Table 3-2: Lab made polymers identification.**

Polymer	Specifications	Provider
SIBS 0		Lab made
SIBS 88 1% graphene oxide		Lab made
SIBS 88 3% graphene oxide		Lab made
SEBS 81.4		Lab made
PS <sub>15</sub> - <i>b</i> -PEEM <sub>60</sub> - <i>b</i> -PTBAM <sub>25</sub> - <i>b</i> -PEEM <sub>60</sub> - <i>b</i> -PS <sub>15</sub>	*	Lab made
PS <sub>25</sub> - <i>b</i> -PEEM <sub>60</sub> - <i>b</i> -PTBAM <sub>15</sub> - <i>b</i> -PEEM <sub>60</sub> - <i>b</i> -PS <sub>25</sub>	*	Lab made
PEEM <sub>60</sub> - <i>b</i> -PTBAM <sub>15</sub> - <i>b</i> -PEEM <sub>60</sub>	*	Lab made
PTBAM		Lab made
PEEK		Lab made
PEGMEM 30% PS		Lab made
PEGMEM 8% alternated		Lab made
PEGMEM 8% block		Lab made

\* PS: polystyrene, PEEM: poly 2-Ethoxyethyl methacrylate, PTBAM: poly 2-(tert-butylamino) ethyl methacrylate and the subscript is the block composition in wt%.

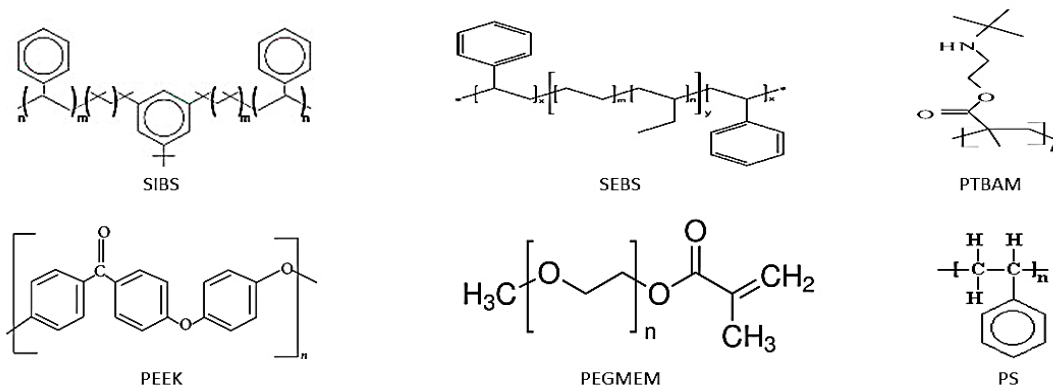


**Figure 3.2-Chemical structures of lab made analyzed polymers.**

Different solvents were needed to dissolve the polymers and prepare the required samples.

Polymers differed from others in their solubility level, so the employed solvents were:

Chlorobenzene, Toluene, Hexyl Alcohol and Sulfuric acid. The solvents used for the sample's preparation are listed on Table 3-3:

**Table 3-3: Solvents identification list.**

<b>Solvent</b>	<b>Specification</b>	<b>Provider</b>
Chlorobenzene	99.8% anhydrous	Sigma-Aldrich
Toluene	Certified ACS	Fisher Chemical
Hexyl alcohol	98% pure	Acros Organics
Sulfuric Acid	ACS reagent (95%-98%)	Sigma-Aldrich

### **3.2 Sample preparation**

All samples were made to have a concentration of 1% wt/wt. A minimum of two replicates were made for each polymer. The procedure for the sample's preparation was the following:

1. The appropriate solvent for the polymer was chosen based on literature reports and knowledge on their respective chemical nature.
2. An amount of solvent was set (3ml – 5ml).
3. The polymer was weighed to achieve a 1% wt/wt solution. Thee unique exceptions were SEBS 81.4, PTBAM and PEEK, due to solubility and polymer quantity issues.
4. All samples were stirred 4 hours and heated at 70°C.
5. Samples were stored protecting them from sunlight.

On Table 3-4 is listed the information for each sample preparation.

**Table 3-4: Analyzed polymers solutions data.**

Polymer	Weighed (g)	Solvent	Solvent amount (ml)	wt %
P3HT	0.0363	CIBz	3.00	1.08
Polyaniline	0.0345	CIBz	3.00	1.03
Poly(tetrafluoroethylene)	0.0339	CIBz	3.00	1.01
SIBS 0	0.0450	CIBz	4.00	1.00
SIBS 88 1% graphene oxide	0.0347	Tol/Hex*	4.00	1.00
SIBS 88 3% graphene oxide	0.0265	Tol/Hex*	3.00	1.02
SEBS 81.4	0.0142	Tol/Hex*	5.00	0.33
PTBAM	0.0345	Sulfuric Acid	3.50	0.53
PEEK	0.0314	Sulfuric Acid	3.50	0.49
PS <sub>15</sub> - <i>b</i> -PEEM <sub>60</sub> - <i>b</i> -PTBAM <sub>25</sub> - <i>b</i> -PEEM <sub>60</sub> - <i>b</i> -PS <sub>15</sub>	0.0350	CIBz	3.00	1.04
PS <sub>25</sub> - <i>b</i> -PEEM <sub>60</sub> - <i>b</i> -PTBAM <sub>15</sub> - <i>b</i> -PEEM <sub>60</sub> - <i>b</i> -PS <sub>25</sub>	0.0355	CIBz	3.00	1.05
PEEM <sub>60</sub> - <i>b</i> -PTBAM <sub>15</sub> - <i>b</i> -PEEM <sub>60</sub>	0.0362	CIBz	3.00	1.08
PEGMEM 30% PS	0.0449	CIBz	4.00	1.00
PEGMEM 8% alternated	0.0454	CIBz	4.00	1.01
PEGMEM 8% block	0.0450	CIBz	4.00	1.00

\*For these samples a ratio of 85% Toluene:15% Hexanol was used.

### 3.3 UV-Vis Analysis

The optical absorption tests were made using a Vernier SpectroVis Plus Spectrophotometer. All the samples were evaluated from 380 nm to 950 nm. In Figure 3.3 is presented a model of the employed spectrophotometer. The light sources for this equipment are a tungsten incandescent bulb and a LED based lamp. More information

about equipment specifications can be obtained at the manufacturer's page.<sup>99</sup> The absorbance data were managed with a compatible program for this equipment called LoggerPro®.



**Figure 3.3-Vernier SpectroVis Plus Spectrophotometer used for UV-Vis tests.<sup>99</sup>**

Once the absorbance spectrum for each polymer was obtained, in order to estimate each bandgap, some calculations were performed. In first place, the optical absorption coefficient ( $\alpha$ ) was calculated using Equation 3-1:

$$\alpha \text{ (cm}^{-1}\text{)} = 2.03 * \frac{A}{d} \quad (3-1)$$

In this case  $d$  = sample thickness or the light path length (1 cm).

The wavelength needs to be converted to electron volts (eV) which is the units of the band gap. The relationship between  $\lambda$  (nm) and  $h\nu$  (eV) is:

$$E \text{ (eV)} = h\nu \text{ (eV)} = \frac{hc}{\lambda} \quad (3-2)$$

Here,  $h$  (Planck's constant) =  $4.135667516 \times 10^{-15}$  eV\*s,  $c$  (speed of light) = 299792458 m/s and  $\lambda$  (wavelength) is given in nm.

To estimate the bandgap of some materials, a plot is created. With previously calculated values,  $(\alpha h\nu)^2$  vs  $h\nu$  is plotted for the direct bandgap case. For the indirect case a plot of  $(\alpha h\nu)^{1/2}$  vs  $h\nu$  was made. In order to estimate the bandgap value, the linear portion of the

corresponding plot is extrapolated to the x axis. The process was done by inspection of the Tauc's plot. It consists on drawing a tangent line to the linear portion of the plot and extend it to the x axis. The value where the line cuts the axis is taken as the bandgap value of the polymer.

### 3.4 Radiation absorption and photon flux harvesting estimation

Once the bandgap values were estimated for the polymers, the maximum possible radiation absorption by the polymer can also be estimated. To do it, the AM 1.5 global solar spectrum was fitted and then integrated. The spectrum data was obtained from the National Renewable Energy Laboratory (NREL) page.<sup>56</sup> To perform the integration, a simple Matlab® program was used (Figure 3.2). The obtained fit of the spectrum was inserted into the program and the band gap limits were set from 0.31 eV (4000 nm) to 4.42 eV (280 nm).

```

1 - clear
2 - clc
3 - syms x
4 - f=input('Enter fit for AM 1.5 solar spectrum:');
5 - a=input('start:');
6 - b=input('end:');
7 - Area=int(f,a,b);
8

```

Figure 3.4-Matlab code for calculating the area of the AM 1.5 solar spectrum.

Once the area for the whole spectrum was calculated, and with the band gap values for each polymer, the area of the maximum radiation absorption was calculated. The process was like the previous one, the only difference was the integration limits. This time the AM 1.5 spectrum fit was integrated from the corresponding band gap of the polymer to 4.42 eV. Then, the ratio between the maximum area that the polymer could reach, and the total area were taken.

Also, the photon harvest from solar spectrum that each polymer could have can be estimated. To do so, the AM 1.5 solar spectrum is converted to the cumulative photo flux. This is done by calculating the corresponding energy of photons for each wavelength and then dividing the spectral irradiance by it for every wavelength. To obtain the cumulative photon flux, each value is summed up or they are integrated.

With this spectrum, the percent estimation of photons harvested by each polymer is calculated by taking the ratio of the cumulative photon flux for the polymer-s band gap to the total photon flux.

## 4 RESULTS & DISCUSSION

### 4.1 AM 1.5 solar spectrum calculations

The first procedure needed for the estimation of the radiation and photon flux harvested by each polymer is the estimation of the total area for the ASTM AM 1.5 solar spectrum (Figure 4.1).

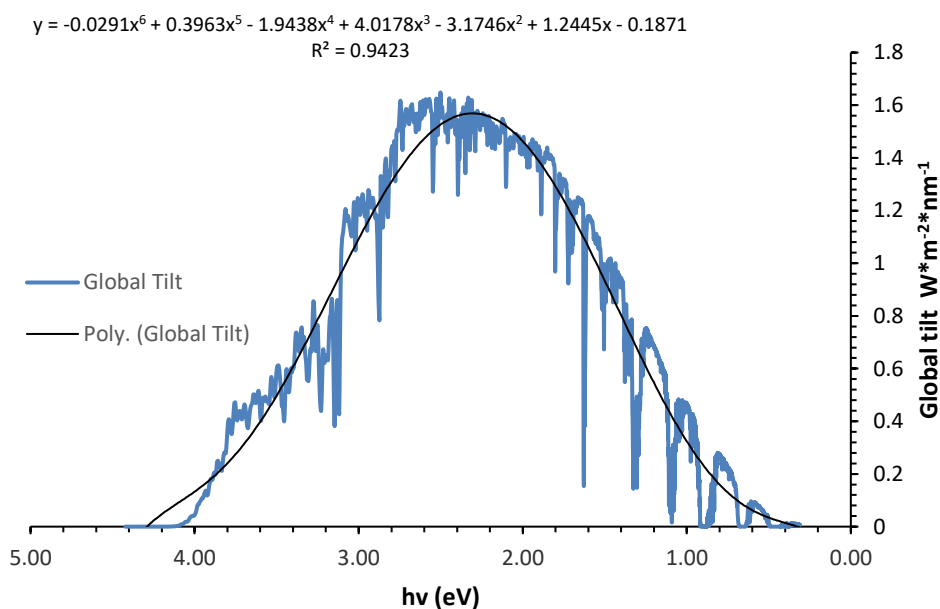


**Figure 4.1-ASTM AM 1.5 fitted solar spectrum.**

The fit approximation was made using a polynomial fit of sixth order (Figure 4.1). This fit was then integrated using Matlab (as explained on the methodology) and the resultant area was  $3.0021 \text{ W*eV/m}^2*\text{nm}$ . Then the spectrum was converted into photon flux. The resultant photon flux is shown on Figure 4.2.

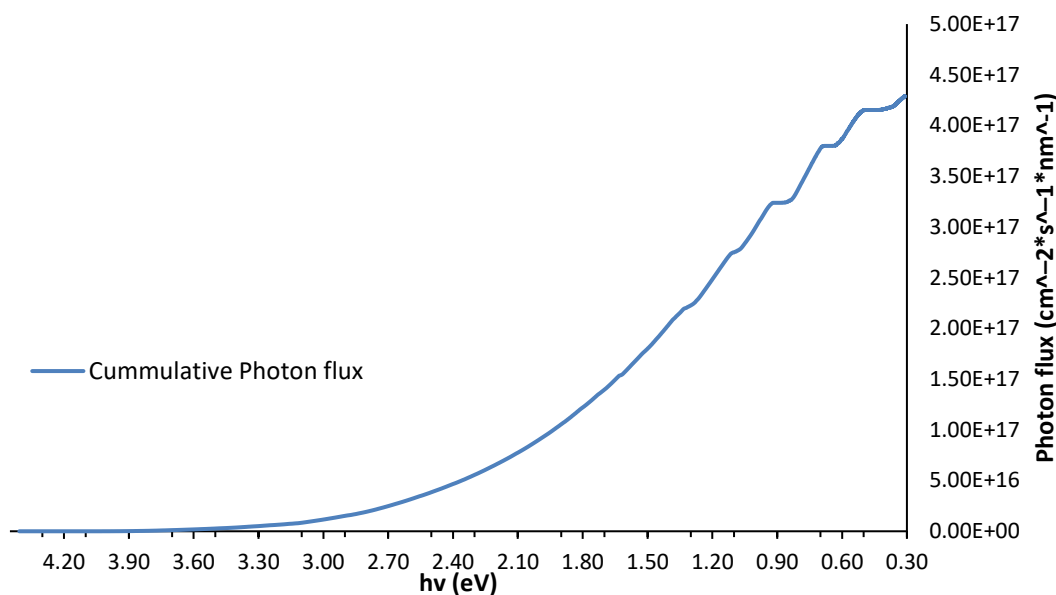


**Figure 4.2-Cumulative photon flux calculated from ASTM AM1.5 solar spectrum.**

With this data the corresponding ratios for radiation and photon flux harvest were calculated as a function of the polymer's band gap.

## **4.2 P3HT, Polyaniline and PTFT**

The first analyzed polymers were the commercial ones. Absorbance graph for these polymers is presented on the Appendix (Figure 7.1-Normalized absorbance for P3HT, PTFE and Polyaniline). With these polymers the band gap calculation approach was tested, and the results were compared with published values. The direct band gap was plotted first. The resultant values can be observed on Figure 4.3.

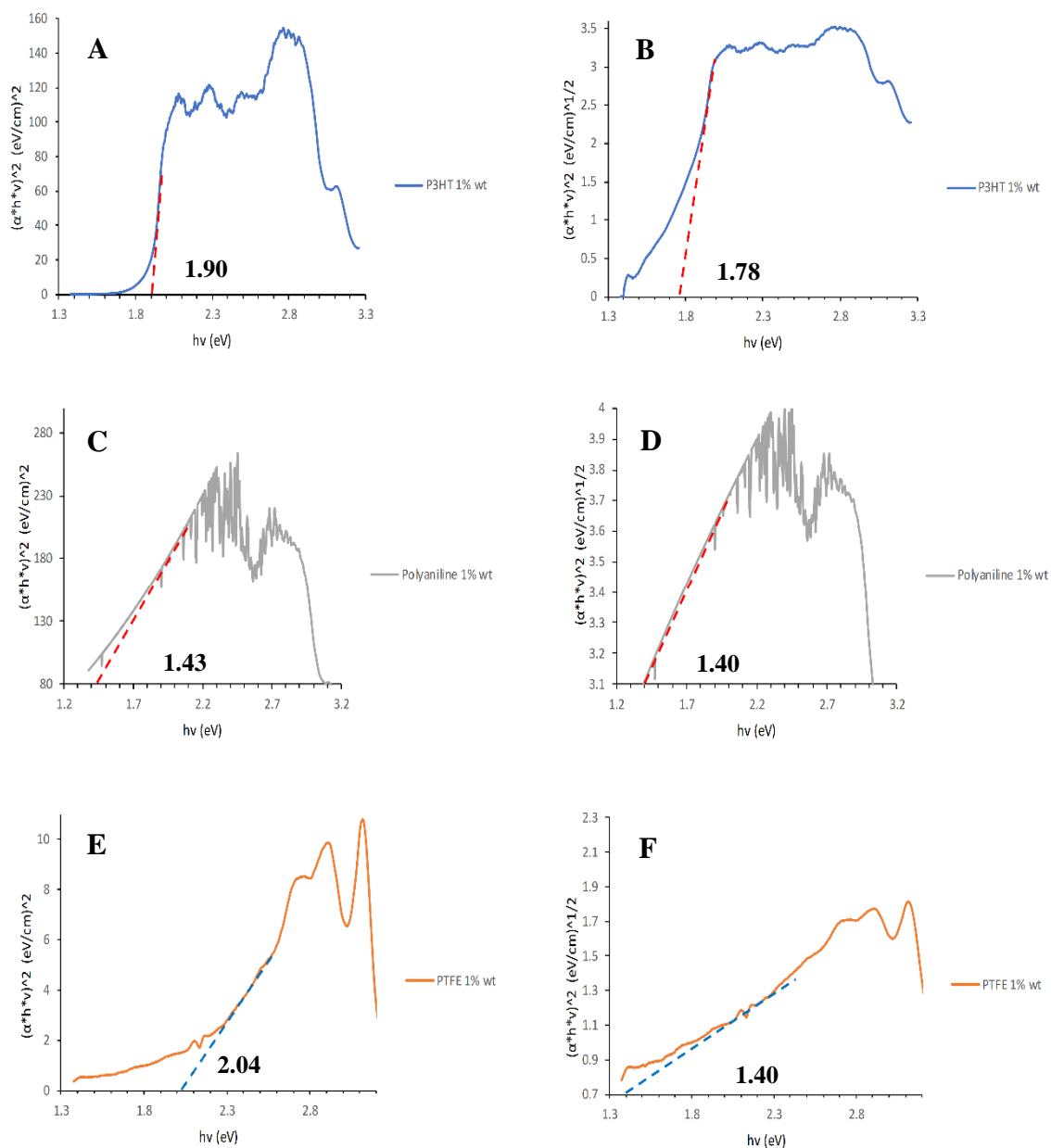


**Figure 4.3-Band gap estimation for commercial polymers. A - P3HT direct band gap. B- P3HT indirect band gap. C- Polyaniline direct band gap. D- Polyaniline indirect band gap. E- PTFE direct band gap. F- PTFE indirect band gap.**

From this first run of calculations the obtained values for the polymers were the following (Table 4-1).

**Table 4-1: Band gap values from Tauc plot for P3HT, Polyaniline and PTFE.**

Polymer	Eg (eV)		Reported (eV)	Error (%)	
	Direct	Indirect		Direct	Indirect
P3HT	1.9	1.78	1.96 <sup>100</sup>	0	6.32
Polyaniline	1.43	1.4	1.50 <sup>101</sup>	4.67	6.67
PTFE	2.04	1.4	1.50 <sup>102</sup>	36.00	6.67

The results for the commercial polymers give a good orientation for the adequateness of the method employed. P3HT has been extensively studied. The reported values vary from 1.90 eV to 1.96 eV and the theory suggest that it is a direct band gap material.<sup>100</sup> These values are near the obtained value and confirms the procedure. Similar accuracy was obtained for Polyaniline. For this polymer, the literature suggests a direct band gap value of 1.5 eV.<sup>101</sup> Finally, for PTFE, the direct estimation deviated from the reported value, however, studies like the ones performed by Mishra et al., supports the fact of an indirect band gap structure for this polymer.<sup>102</sup>

With the appropriated values according to literature, the calculated radiation and photon flux harvest for these polymers is presented on Table 4-2.

**Table 4-2: Radiation and photon flux possible achievable percentages for P3HT, Polyaniline and PTFE.**

<b>Polymer</b>	<b>E<sub>g</sub> (eV)</b>	<b>Possible capturable radiation %</b>	<b>Possible photon flux harvest %</b>
P3HT	1.90	40.92	24.38
Polyaniline	1.43	65.07	45.54
PTFE	1.40	66.86	47.35

The results obtained for P3HT matches the calculated values for photon harvesting. Kroon et al. calculated the photon harvesting percent at 22.4%.<sup>80</sup> Our estimated value for this same polymer was 24.38%, which is not far away from the reported value. This value is considered a poor harvested choice, since it limits the absorbance to wavelengths below 650 nm, which is less than the half of the entire AM1.5 spectrum. For Polyaniline and PTFE, the photon harvesting percentages almost reach the 50%. It has been stated that for single absorbing polymers (commonly acceptors), the optimal band gap value is within the values of these polymers.<sup>103</sup> However, for combined blends of polymers the optimal band gap has been estimated on a range between 1.3 eV-1.9 eV.

An important observation that can be made is the difference between the radiation and photon flux percentages. The major part of the solar radiation is found on the visible and the first part of the near infrared region on the electromagnetic spectrum. However, the photon flux of the solar spectrum does not decrease when it approaches 4000 nm. For that reason, the polymers absorbing on the visible region will absorb less photons than near infrared absorbing polymers, even though they match the strongest part of the solar

spectrum.

### 4.3 SIBS and SEBS 81.4

SIBS is a polymer with a wide variety of applications. It has been used on the adhesives and sealer market, medical treatments and for the fuel cells as proton exchange membranes.<sup>6</sup> This last application was the one initially planned or the analyzed polymers.

For these polymers, only a few optical properties have been reported; however, it is known that they have a refractive index (n) of 1.525-1.535.<sup>104</sup> Using that parameter  $E_g$  values can be estimated from empirical relations. Many relations have been presented during the years, but for this work, the one presented by Anani et al. was employed.<sup>105</sup>

The relation is as follows:

$$n^4 = 1 + \frac{A}{E_g^2} \quad (4-1)$$

Where n is the refractive index,  $E_g$  is the materials band gap and A is a fit parameter equal to 40.8 eV.

Absorbance graph for these polymers is presented on the Appendix (Figure 7.2-Normalized absorbance for SIBS and SEBS polymers). The obtained values for direct and indirect band gap are shown on Figure 4.4. Compared to previously presented values for commercial

polymers, SIBS 0 estimated band gap, seems to draw away next to the 3 eV.

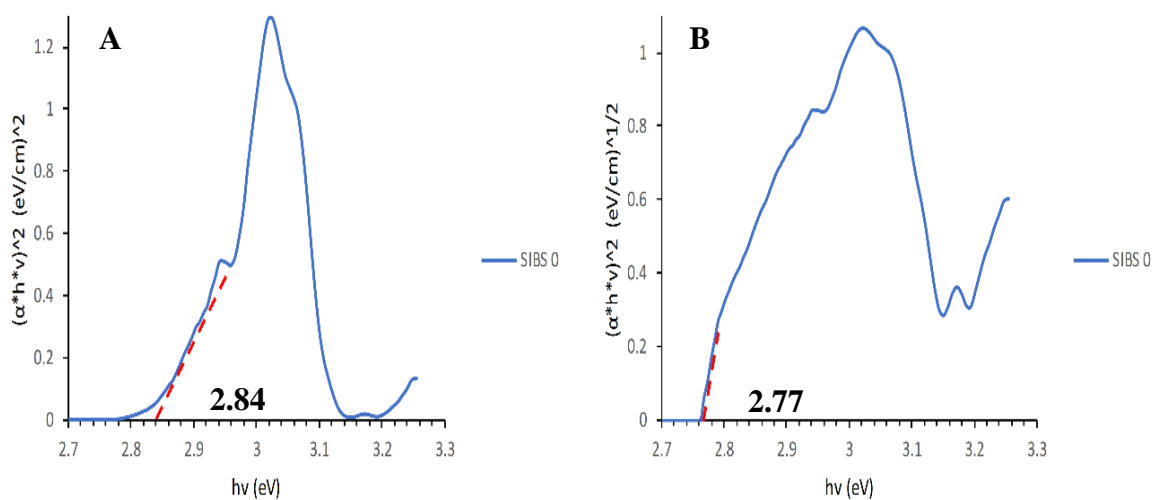


**Figure 4.4-A) Direct band gap estimation for SIBS 0. B) Indirect band gap estimation for SIBS 0.**

When it is compared to the band gap prediction made with the Anani et al. relation, the value appears to be near the correct value (only if the refraction index is taken in consideration). The estimated value differs from the calculated ones within the range of 10% error (Table 4-3).

**Table 4-3: SIBS 0 band gap estimation values and comparison with estimation using Anani et al. relation.**

Polymer	Eg (eV)		Predicted (eV)	Error (%)	
	Direct	Indirect		Direct	Indirect
SIBS 0	2.84	2.77	3.07	7.40	9.68

Starting from this point (no sulfonation) other samples of SIBS polymers were evaluated. Obtained band gap values for these polymers are presented on Figure 4.5.

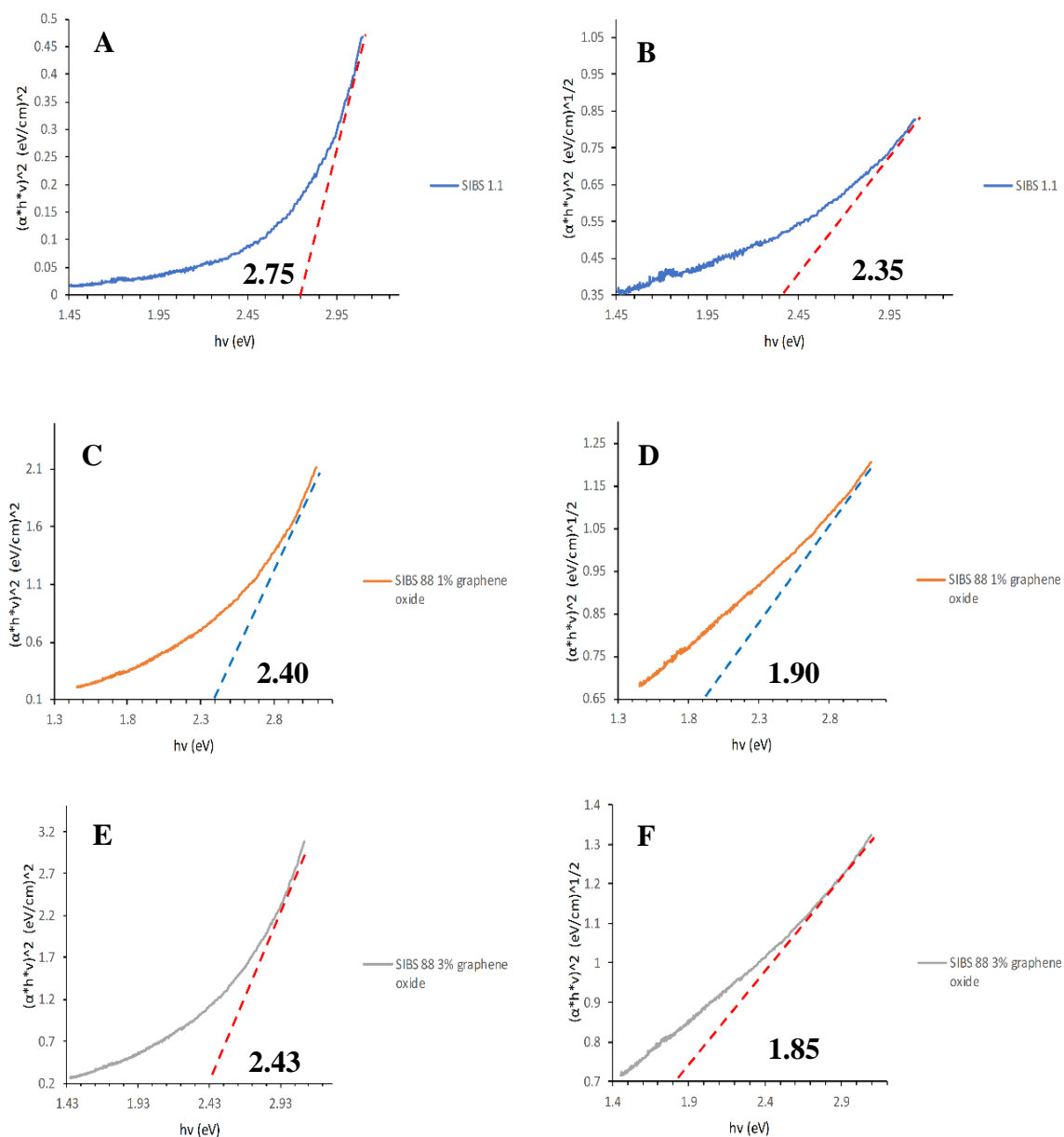


**Figure 4.5-A-B: Direct and indirect band gap for SIBS 1.1. C-D: Direct and indirect band gap for SIBS 88 1% graphene oxide. F-E: Direct and indirect band gap for SIBS 88 3% graphene oxide.**

From these results is important to note that the band gap for each polymer decreased in respect to SIBS 0. Two important contributions come into play for consideration. The first one is the effect of sulfonation on the polymer. From a SIBS 0 direct band gap of 2.84 eV,

values of 2.40 eV and 2.43 eV were obtained. It suggests an important reduction on the polymer band gap about 0.4 eV. This behavior is indirectly supported by the work of Jung et al.<sup>106</sup> They studied the effect of sulfonation on polystyrene and found a similar relation but with respect of the refractive index. For their research, refractive index decreased approximately by 0.06 for the complete sulfonated polymer, when compared to pure polystyrene. Also, this behavior is supported by Liao et al., in their work with sulfonated polymers such as polyaniline.<sup>107</sup> They found out a sixth order enhanced conductivity for sulfonated samples when compared to normal polyaniline.

SIBS 88 polymers also have the contribution of graphene oxide; however, the effect of this contribution cannot be explained based on results. Some studies reveal non-conducting properties for graphene oxide composites. It behaves as an insulator, but when it is reduced or sulfonated its electrical conductivity increases.<sup>108, 109</sup> It may be a factor for these SIBS 88 polymers, however this deserves further study.

Along with these polymers SEBS 81.4 was also studied. For this case the results show that band gap were 2.75 eV and 2.45 eV for the direct and indirect gaps respectively (Figure 4.6). Although it cannot be compared with non-sulfonated SEBS, its values are like SIBS 1.1. It may be related to the same behavior of band gap reduction in SIBS polymers.

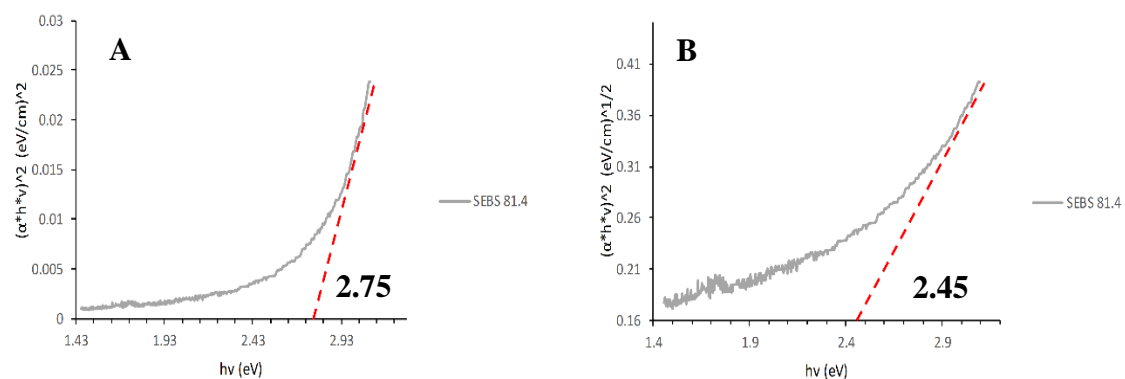


**Figure 4.6-SEBS 81.4 direct and indirect band gap (A and B respectively).**

Below is presented a summary of the polymer's band gap results (Table 4-4).

**Table 4-4: Band gap results for SIBS and SEBS 81.4 runs.**

Polymer	E <sub>g</sub> (eV)		Predicted (eV)	Error (%)	
	Direct	Indirect		Direct	Indirect
SIBS 0	2.84	2.77	3.07	7.40	9.68
SIBS 1.1	2.75	2.35	NA	NA	NA
SIBS 88 1% graphene oxide	2.40	1.90	NA	NA	NA
SIBS 88 3% graphene oxide	2.43	1.85	NA	NA	NA
SEBS 81.4	2.75	2.45	NA	NA	NA

With the obtained band gap values the possible achievable radiation and photon flux percent is shown on Table 4-5.

**Table 4-5: Radiation and photon flux harvest percent for SIBS polymers and SEBS 81.4.**

<b>Polymer</b>	<b>E<sub>g</sub> (eV) (Direct/Indirect)</b>	<b>Possible capturable radiation %</b>	<b>Possible photon flux harvest %</b>
SIBS 0	2.84/2.77	8.90/10.40	4.06/4.84
SIBS 1.1	2.75/2.35	10.86/22.59	5.08/11.78
SIBS 88 1% graphene oxide	2.40/1.90	20.95/40.92	10.78/24.38
SIBS 88 3% graphene oxide	2.43/1.85	20.02/43.41	10.22/26.29
SEBS 81.4	2.75/2.45	10.86/19.4	5.08/9.85

From the previous data it is readily noted that none of these polymers is close to the percentages reported by the commercial polymers. As discussed, SIBS 88 samples indicated the lowest band gap values; however, the limited possibility of radiation and photons capture, do not make them candidates for absorbing polymers. However, this may not inhibit completely their use since these values are near the band gap value of one of the most used acceptors in OSCs field; PCBM. This polymer is a functionalized fullerene who is catalogued as a n-type semiconductor. Its band gap is 2.40 eV. The similarity between band gaps may suggest a similar behavior in the exciton dissociation process.

#### **4.4 PEEK, PTBAM and block polymers**

The second group of analyzed polymers started with PEEK. This polymer is recognized as one of the most stable polymers. It stands out for its chemical stability, being affected only by strong acids and bases, and as well for its thermal stability.

Its refractive index is 1.67.<sup>110</sup> With this value the approximated  $E_g$  was 2.45 eV. When the corresponding data were plotted, the obtained value for PEEK's band gap were 2.50 eV and 2.30 eV for direct and indirect cases respectively. Plots are shown on Figure 4.7.

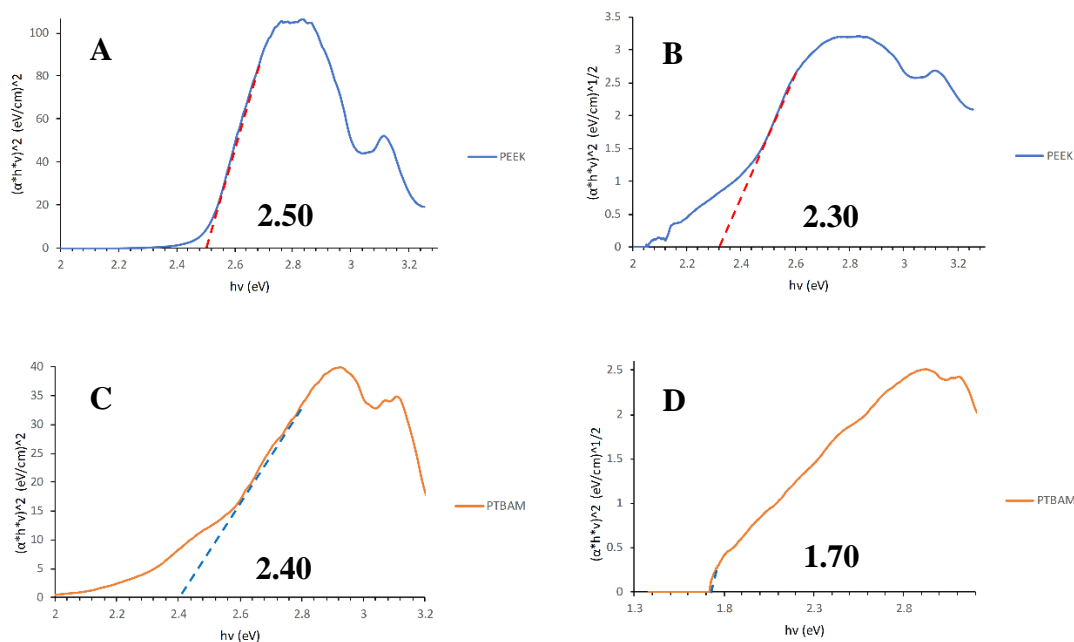


**Figure 4.7-PEEK direct and indirect band gap (A-B). PTBAM direct and indirect band gap (C-D).**

For PTBAM, the resultant band gaps were 2.40 eV and 1.70 eV. This polymer's available information about conductivity is not abundant. Most works have focused on its antimicrobial properties and the reinforcement of materials.<sup>111</sup> Some chemical providers provide a refractive index of 1.43 for the 2-(*t*-buthylamino)ethyl methacrylate monomers.<sup>112</sup> This value suggests a band gap value over 3 eV for monomers, however the exact value for polymers is not reported. With all this information, the preliminary conclusions for PTBAM are that it is not expected to be a good semiconductor.

Comparing the structure of PEEK with PTBAM (Figure 3.2-Chemical structures of lab made analyzed polymers.), it is easy to note that PEEK is a more conjugated polymer than PTBAM.

According to the literature, it promotes the semiconductor behavior by reducing the band gap of the polymer. It leads the thinking line to not expect any significant effect on electron conduction, besides the fact that PTBAM have a PCBM like band gap.

**Table 4-6: Radiation and photon flux estimated harvest percent for PEEK and PTBAM.**

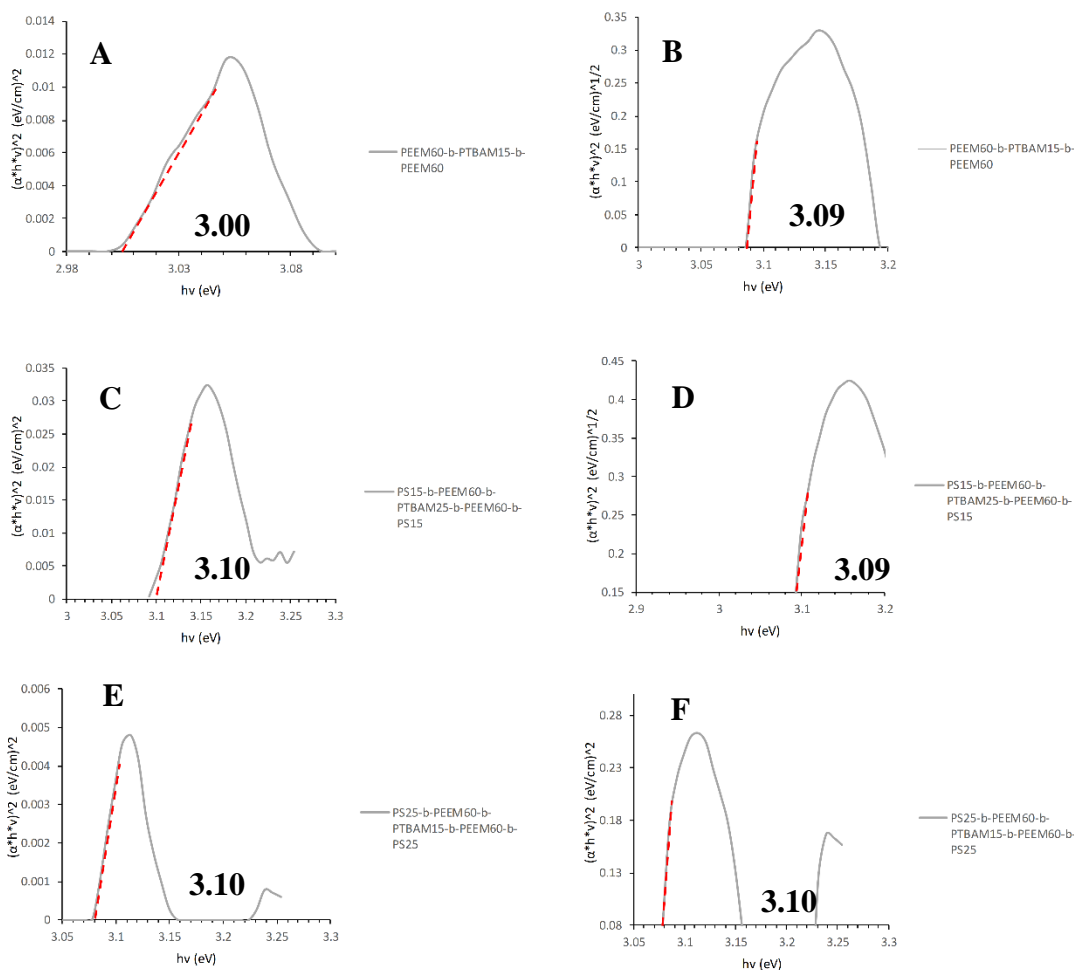
<b>Polymer</b>	<b>Eg (eV) (Direct/Indirect)</b>	<b>Possible capturable radiation %</b>	<b>Possible photon flux harvest %</b>
PEEK	2.50/2.30	17.86/24.44	8.95/12.93
PTBAM	2.40/1.72	20.95/49.93	10.78/31.58

Table 4-6 presents the estimated values for radiation and photon flux percentages. The maximum values do not exceed 20% for the direct band gap possibility and 50% for the indirect case. The most probable case for these polymers is the direct case, due to the planarity of their structure. In this situation, the values agree with the most used acceptors for OSCs.

In addition to these two polymers, but related, three block copolymers were analyzed. The blocks used for these copolymers were PEEM, PTBAM and PS. Obtained bandgap are shown on Figure 4.8.

From the obtained values an important observation is to note that the variation on the results is not high. Initially for the PEEM60-b-PTBAM15-b-PEEM60 band gap values were 3.00 eV and 3.09 eV. This value is far away from the 2.40 eV values for SIBS 88 and from the PCBM reported values. For this case PTBAM is not the abundant block and this can lead us to various conclusions. In the first place, the PEEM polymer does not seem to be a good semiconductor material. In second place, PTBAM does not seem to have enough

influence to lower the band gap of this copolymer or this may support the idea that PTBAM does not behave as a semiconductor.



**Figure 4.8-Direct and indirect band gap for: PEEM60-b-PTBAM15-b-PEEM60 (A-B), PS15-b-PEEM60-b-PTBAM25-b-PEEM60-b-PS15 (C-D) and PS25-b-PEEM60-b-PTBAM15-b-PEEM60-b-PS25 (E-F).**

The other two polymers analyzed were like the first one with exception of the incorporation of PS. Polystyrene is a very commonly employed polymer for many applications today. Literature reports discrepancies on its refractive index. Values are presented in the range of 1.20-1.59.<sup>113, 114</sup> With these values, is not a surprising to find publications reporting band

gaps near the 2.70 eV, associated to doping and treatments, and far beyond 4 eV, associated to insulator behavior.

This last behavior explains the results for the copolymers analyzed. For both cases, values were higher for the direct case than compared to the PEEM-PTBAM polymer. The indirect case does not change significantly. Even though the literature says that the planar structures favors the band gap lowering, the observed reduction is not significant, in fact it increased.

**Table 4-7: Estimated radiation and photon flux harvest for PEEK, PTBAM and PEEM-PTBAM-PS co polymers.**

<b>Polymer</b>	<b>Eg (eV) (Direct/Indirect)</b>	<b>Possible capturable radiation %</b>	<b>Possible photon flux harvest %</b>
PEEK	2.50/2.30	17.86/24.44	8.95/12.93
PTBAM	2.40/1.72	20.95/49.93	10.78/31.58
PEEM60-b-PTBAM15-b- PEEM60	3.00/3.09	6.18/4.78	2.71/2.04
PS15-b-PEEM60-b- PTBAM25-b-PEEM60-b- PS15	3.10/3.09	4.55/4.78	1.94/2.04
PS25-b-PEEM60-b- PTBAM15-b-PEEM60-b- PS25	3.08/3.08	4.9	2.1

The results are summarized on Table 4-7. A huge contrast is observed between the capturable radiation and photon flux harvesting. Radiation fall to an under 7% limit for the copolymers and under 3% for photon flux reaching. These values do not represent any potential useful properties for OSC; however, it may lie on the OLEDs category.<sup>115</sup>

In contrast, PEEK and PTBAM may work as acceptor polymers for some OSCs, if other parameters are favored as well. In fact, PEEK has been found to be an excellent conductor material when it is doped with carbon black and graphene.<sup>116, 117</sup> However an important issue to study on these polymers will be its stability in presence of solar radiation. Absorbance graphs for these polymers is presented on the Appendix (Figure 7.3-Normalized absorbance for PEEK, PTBAM and block polymers).

#### **4.5 PEGMEM polymers**

Poly (ethylene glycol) methyl ether methacrylate polymers have a variety of applications. Some of them goes from biological activity to the synthesis of block copolymers. One positive trait that make these polymers suitable for use is the hydrophilicity. The polymer exhibits a long linear chain made by carbons and oxygen who favors the crosslinks with other materials and the solubility of these materials.

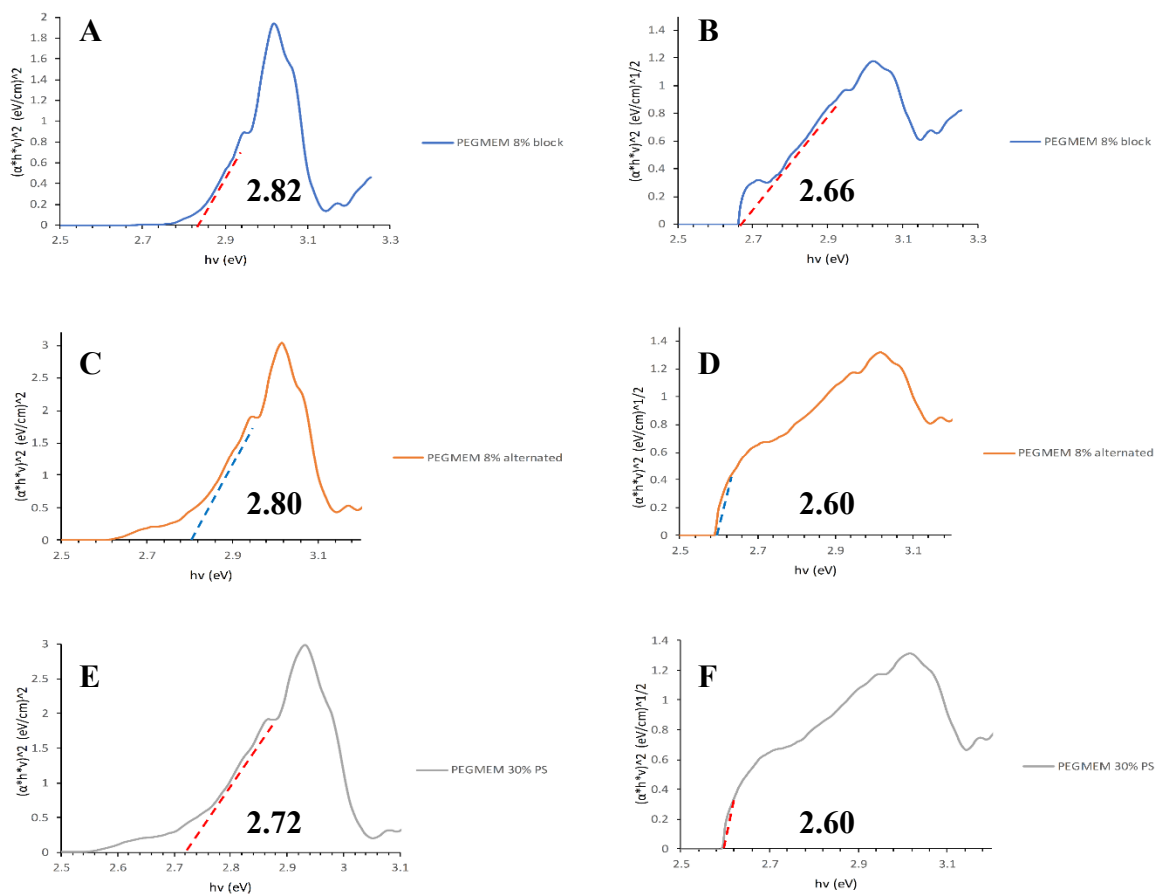


**Figure 4.9-Direct and indirect band gap calculations for PEGMEM 8% block (A-B), PEGMEM 8% alternated (C-D) and PEGMEM 30% PS (E-F).**

Figure 4.9 shows the band gap values obtained for the three PEGMEM polymers analyzed. The obtained results were 2.82 eV and 2.66 eV for the 8% block sample, 2.80 eV and 2.60 eV for the 8% alternated sample and, 2.72 eV and 2.60 eV, for the 30% PS sample. From literature and suppliers, the refractive index for PEGMEM is approximately 1.50.<sup>118</sup> With this value and the Anani approximation, the estimated value for PEGMEM should be near 3.17 eV. With this approximation the error percentages for the calculations are shown next on Table 4-8.

**Table 4-8: Calculated band gap values for PEGMEM polymers.**

Polymer	E <sub>g</sub> (eV)		Predicted (eV)	Error (%)	
	Direct	Indirect		Direct	Indirect
PEGMEM 8% block	2.82	2.66	3.17	11.02	16.06
PEGMEM 8% alternated	2.80	2.60	3.17	11.65	17.96
PEGMEM 30% PS	2.72	2.60	-	-	-

In first place, the predicted  $E_g$  value and the calculated ones, difference exceed the 10% range for both cases. However, the direct and gap calculations are near the acceptable limit, which may suggest a direct semiconductor behavior like other materials. In second place, a reduction on the band gap is observed mainly for the direct case. The contrast between the block and alternated structures do not present any significant difference, but contrary to that, the polystyrene presence seems to have an effect. When compared to the block and alternated arrangements, seems to be a reduction of near 0.10 eV. As discussed on previous section PS, is a very versatile material which will be no surprise that influence band gap lowering at some level.

From these results the predicted radiation and photon flux harvested are shown in Table 4-9 below.

**Table 4-9: Possible radiation and photon flux harvest for PEGMEM polymers.**

<b>Polymer</b>	<b>E<sub>g</sub> (eV) (Direct/Indirect)</b>	<b>Possible capturable radiation %</b>	<b>Possible photon flux harvest %</b>
PEGMEM 8% block	2.82/2.66	9.28/13.19	4.26/6.33
PEGMEM 8% alternated	2.80/2.60	9.69/14.90	4.47/7.27
PEGMEM 30% PS	2.72/2.60	11.63/14.90	5.48/7.27

From results shown, the values are not good enough to be considered as acceptor materials. For the direct case the radiation capture does not exceed the 12% and the photon flux harvest the 6%. These values are far away from the ones obtained on SIBS 88, PEEK and PTBAM (2.40-2.50). The crosslinks favoring may be a reason for high band gap values. Literature states that planar structures and conjugation contribute on the band gap lowering process. This polymer possesses a linear portion on his chain that could behave as a planar structure and favor the stacking. Also, the polymer alternation of C-C bonds with oxygen generates a similar situation like in conjugated polymers. However, if a polymer makes links with diverse parts of itself some rich electron regions could end trapped. This idea is supported by Rumer and McCulloch. In their work they present the role played by crosslinks on the OSC efficiency. On this work, one of the important conclusions is that crosslinks should be made on specific areas of polymers looking for not perturb the conjugated system of a molecule and his critical structure.<sup>119</sup> Absorbance graph for these polymers is presented on the Appendix (Figure 7.4-Normalized absorbance for EGMEM polymers).

## 5 CONCLUSION & RECOMMENDATIONS

The main objectives of this work were achieved. Four polymers groups were studied to estimate their respective bandgap values and radiation harvest percentages. The methodology was supported by the P3HT, Polyaniline and PTFE results. The estimated values for these polymers had an error within the range of 3.06%-6.67%, and their estimated photon flux capture agree with reported values on literature. For the laboratory prepared polymers, the best results were obtained from SIBS group, PEEK and PTBAM. SIBS 88 (with graphene oxide) polymers resulted on having a bandgap between 2.40eV-2.43eV (direct case). These polymers estimated radiation capture was from 20 to 21 percent and the photon flux harvest from 10 to 11 percent. The PEEK and PTBAM cases shown band gaps of 2.50eV and 2.40eV respectively, and the radiation and photon flux harvest were on the range of 17%-20% and 8%-10% for each one respectively.

Based on the results, a recommendation will be to employ PEEK on future OSCs studies. Taking advantage of the stability and mechanical properties of this polymer could be possible to use it to improve solar cells characteristics, as well as efficiency. In a second place, SIBS 88 polymers could be employed as acceptors on heterojunction devices. However, studies must be conducted on the stability of these polymers.

Future work on this area could include the polymers test for challenges present on a photovoltaic device such as: weathering, stability and water exposure. Also, another

study area could be the effect of sulfonation and graphene doping on different polymers in order to band gap tuning for diverse purposes.

## 6 REFERENCES

- (1) Commission of the European Communities. Green Paper: A European Strategy for Sustainable, Competitive and Secure Energy., 2006.
- (2) Intergovernmental Panel on Climate Change. Climate Change 2007: The Physical Science Basis., 2007.
- (3) The Guardian. Background: What Caused the 1970s Oil Price Shock? March 3, 2011.
- (4) Kamp, L.; Smits, R.; Andriess, C. Notions on Learning Applied to Wind Turbine Development in the Netherlands and Denmark. *Ener Poli* **2004**, *32*, 1625–1637.
- (5) The Economist. Power Buoys: Electricity from Waves. May 17, 2001, pp 78–79.
- (6) Becquerel, E. Memoire Sur Les Effects d'Electriques Produits Sous l'Influence Des Rayons Solaires. *Comptes Rendus de l'Academie des Sciences* **1839**, *9*, 561–567.
- (7) Smith, W. Effect of Light on Selenium During the Passage of An Electric Current\*. *Nature* **1873**, *7*, 303.
- (8) Adams, W.G. ; Day, R.E. The Action of Light on Selenium. *Proc. R. Soc. Lond.* **1877**, *25*, 113–117.
- (9) Fritts, C. On a New Form of Selenium Photocell. *American Journal of Science* **1883**, *26*.
- (10) Green, M. A. Photovoltaics: Coming of Age.; 21st IEEE Photovoltaic Specialists Conference: Orlando, USA, 1990; pp 1–8.
- (11) Siemens, W. On the Electromotive Action of Illuminated Selenium, Discovered by Mr. Fritts, of New York. *Van Nostrands Eng. Mag.* **1885**, *32*, 514–516.
- (12) Perlin, J. The Invention Of The Solar Cell. *Popular Science*. April 22, 2014.
- (13) Klassen, S. The Photoelectric Effect: Reconstructing the Story for the Physics Classroom.,. *Sci. Educ.* **2011**, *20*, 719–731. <https://doi.org/10.1007/s11191-009-9214-6>.
- (14) What is the Photoelectric Effect? » Science ABC <https://www.scienceabc.com/pure-sciences/what-explain-photoelectric-effect-einstein-definition-exmample-applications-threshold-frequency.html> (accessed Jan 18, 2019).
- (15) Pochettino, A. Sul Comportamento Foto-Elettrico Dell'Antracene. *Acad. Lincei Rend.* **1906**, *15*, 355–363.
- (16) Volmer, M. Die Verschiedenen Lichtelektrischen Erscheinungen Am Anthracen, Ihre Beziehungen Zueinander, Zur Fluoreszenz Und Dianthracenbildung. *Ann. Physik* **1913**, *40*, 775–796. <https://doi.org/10.1002/andp.19133450411>.
- (17) Grondahl, L.O. The Copper-Cuprous-Oxide Rectifier and Photoelectric Cell. *Review of Modern Physics* **1993**, *5*, 141.
- (18) Nix, F.C.; Trepto, A.W. A Thallous Sulphide Photo EMF Cell. *Journal Opt. Society of America* **1939**, *29*, 457.
- (19) Chaplin, D.M.; Fuller, D.S.; Pearson, G.L. A New Silicon P-n Junction Photocell for Converting Solar Radiation into Electrical Power. *Journal of Applied Physics* **1954**, *25*, 676–677.

- (20) Mathielson, A.M.; Robertson, J.M.; Sinclair, V.C. The Crystal and Molecular Structure of Anthracene. I. X-ray Measurements. *Acta Cryst* **1950**, *3*, 245–250. <https://doi.org/10.1107/S0365110X50000641>.
- (21) Chaiken, R. F.; Kearns, D.R. Intrinsic Photoconduction in Anthracene Crystals. *J. Chem. Phys.* **1966**, *45*, 451. <https://doi.org/10.1063/1.1727446>.
- (22) Tang, C. W.; Albrecht, A. C. Transient Photovoltaic Effects in Metal-Chlorophyll-a-Metal Sandwich Cells. *Journal of Chemical Physics* **1975**, *63* (2), 953–961.
- (23) Ballschmiter, K.; Katz, J.J. Chlorophyll-Chlorophyll and Chlorophyll-Water Interactions in the Solid State. *Biochim. Biophys. Acta* **1972**, *256* (2), 307–327. [https://doi.org/doi.org/10.1016/0005-2728\(72\)90062-X](https://doi.org/doi.org/10.1016/0005-2728(72)90062-X).
- (24) Tang, C.W. Two-layer Organic Photovoltaic Cell. *Appl. Phys. Lett.* **1986**, *48* (2), 183–185. <https://doi.org/doi.org/10.1063/1.96937>.
- (25) Cozzens, R.F. Chapter 3: Electrical Conductivity. In *Electrical Properties of Polymer*; Academic Press: New York, 1982; p 93.
- (26) Weinberger, B. R.; Akhtar, M.; Gau, S. C. Polyacetylene Photovoltaic Devices. *Synth. Met.* **1982**, *4* (3), 187–197. [https://doi.org/10.1016/0379-6779\(82\)90012-1](https://doi.org/10.1016/0379-6779(82)90012-1).
- (27) Glenis, S.; Tourillon, G.; Garnier, F. Influence of the Doping on the Photovoltaic Properties of Thin Films of Poly-3-Methylthiophene. *Thin Solid Films* **1986**, *139* (3), 221–231. [https://doi.org/10.1016/0040-6090\(86\)90053-2](https://doi.org/10.1016/0040-6090(86)90053-2).
- (28) Spanggaard, H.; Krebs, F. C. A Brief History of the Development of Organic and Polymeric Photovoltaics. *Sol. Energy Mater. Sol. Cells* **2004**, *83* (2), 125–146. <https://doi.org/10.1016/j.solmat.2004.02.021>.
- (29) Karg, S.; Riess, W.; Dyakonov, V.; Schwoerer, M. Electrical and Optical Characterization of Poly(Phenylene-Vinylene) Light Emitting Diodes. *Synth. Met.* **1993**, *54* (1), 427–433. [https://doi.org/10.1016/0379-6779\(93\)91088-J](https://doi.org/10.1016/0379-6779(93)91088-J).
- (30) Marks, R. N.; Halls, J. J. M.; Bradley, D. D. C.; Friend, R. H.; Holmes, A. B. The Photovoltaic Response in Poly(p-Phenylene Vinylene) Thin-Film Devices. *J. Phys. Condens. Matter* **1994**, *6* (7), 1379–1394. <https://doi.org/10.1088/0953-8984/6/7/009>.
- (31) Antoniadis, H.; Hsieh, B. R.; Abkowitz, M. A.; Jenekhe, S. A.; Stolka, M. Photovoltaic and Photoconductive Properties of Aluminum/Poly(p-Phenyl Vinylene) Interphases. *Synth. Met* **1994**, *62*, 265.
- (32) Nelson, R. C. Sensitization of Photoconductivity in Cadmium Sulfide\*. *JOSA* **1956**, *46* (1), 13–16. <https://doi.org/10.1364/JOSA.46.000013>.
- (33) Sariciftci, N. S.; Smilowitz, L.; Heeger, A. J.; Wudl, F. Semiconducting Polymers (as Donors) and Buckminsterfullerene (as Acceptor): Photoinduced Electron Transfer and Heterojunction Devices. *Synth. Met.* **1993**, *59* (3), 333–352. [https://doi.org/10.1016/0379-6779\(93\)91166-Y](https://doi.org/10.1016/0379-6779(93)91166-Y).
- (34) Tada, K.; Onoda, M.; Nakayama, H.; Yoshino, K. Photocell with Heterojunction of Donor /Acceptor Polymers. *Synth. Met.* **1999**, *102* (1), 982–983. [https://doi.org/10.1016/S0379-6779\(98\)01049-2](https://doi.org/10.1016/S0379-6779(98)01049-2).

- (35) Yu, G.; Heeger, A. J. Charge Separation and Photovoltaic Conversion in Polymer Composites with Internal Donor/Acceptor Heterojunctions. *J. Appl. Phys.* **1995**, *78* (7), 4510–4515. <https://doi.org/10.1063/1.359792>.
- (36) Halls, J. J. M.; Walsh, C. A.; Greenham, N. C.; Marseglia, E. A.; Friend, R. H.; Moratti, S. C.; Holmes, A. B. Efficient Photodiodes from Interpenetrating Polymer Networks. *Nature* **1995**, *376* (6540), 498–500. <https://doi.org/10.1038/376498a0>.
- (37) Rasmussen, S. Low-Bandgap Polymers. In *Encyclopedia of Polymeric Nanomaterials*; Kobayashi, S., Müllen, K., Eds.; Springer Berlin Heidelberg: Berlin, Heidelberg, 2013; pp 1–13. [https://doi.org/10.1007/978-3-642-36199-9\\_5-1](https://doi.org/10.1007/978-3-642-36199-9_5-1).
- (38) Pomerantz, M. Low Band Gap Conducting Polymers. In *Handbook of conducting polymers*; Skotheim, T. A., Elsenbaumer, R. L., Reynolds, J. R., Eds.; Marcel Dekker: New York, 1998; pp 277–309.
- (39) Roncali, J. Synthetic Principles for Bandgap Control in Linear Pi-Conjugated Systems. *Chem. Rev.* **1997**, *97* (1), 173–206.
- (40) Wudl, F.; Kobayashi, M.; Heeger, A. J. Poly(Isothianaphthene). *J. Org. Chem.* **1984**, *49* (18), 3382–3384. <https://doi.org/10.1021/jo00192a027>.
- (41) Brisset, H.; Thobie-Gautier, C.; Gorgues, A.; Jubault, M.; Roncali, J. Novel Narrow Bandgap Polymers from Sp<sup>3</sup> Carbon-Bridged Bithienyls: Poly(4,4-Ethylenedioxy-4H-Cyclopenta[2,1-b;3,4-B']Dithiophene). *J. Chem. Soc. Chem. Commun.* **1994**, *0* (11), 1305–1306. <https://doi.org/10.1039/C39940001305>.
- (42) Halls, J. J. M.; Pichler, K.; Friend, R. H.; Moratti, S. C.; Holmes, A. B. Exciton Diffusion and Dissociation in a Poly(P-phenylenevinylene)/C<sub>60</sub> Heterojunction Photovoltaic Cell. *Appl. Phys. Lett.* **1996**, *68* (22), 3120–3122. <https://doi.org/10.1063/1.115797>.
- (43) Shaheen, S. E.; Brabec, C. J.; Sariciftci, N. S.; Padinger, F.; Fromherz, T.; Hummelen, J. C. 2.5% Efficient Organic Plastic Solar Cells. *Appl. Phys. Lett.* **2001**, *78* (6), 841–843. <https://doi.org/10.1063/1.1345834>.
- (44) Kim, K.; Liu, J.; Namboothiry, M. A. G.; Carroll, D. L. Roles of Donor and Acceptor Nanodomains in 6% Efficient Thermally Annealed Polymer Photovoltaics. *Appl. Phys. Lett.* **2007**, *90* (16), 163511. <https://doi.org/10.1063/1.2730756>.
- (45) Wolfgang, T. Device Physics of Organic Solar Cells. Dissertation, Technischen Universität Dresden: Dresden, Germany, 2011.
- (46) Green, M. A.; Emery, K.; Hishikawa, Y.; Warta, W.; Dunlop, E. D. Solar Cell Efficiency Tables (Version 39). *Prog. Photovolt. Res. Appl.* **2012**, *20* (1), 12–20. <https://doi.org/10.1002/pip.2163>.
- (47) Liang, Y.; Xu, Z.; Xia, J.; Tsai, S.-T.; Wu, Y.; Li, G.; Ray, C.; Yu, L. For the Bright Future—Bulk Heterojunction Polymer Solar Cells with Power Conversion Efficiency of 7.4%. *Adv. Mater.* **2010**, *22* (20), E135–E138. <https://doi.org/10.1002/adma.200903528>.
- (48) Wang, M.; Hu, X.; Liu, P.; Li, W.; Gong, X.; Huang, F.; Cao, Y. Donor–Acceptor Conjugated Polymer Based on Naphtho[1,2-*c*:5,6-*c'*]Bis[1,2,5]Thiadiazole for

- High-Performance Polymer Solar Cells. *J. Am. Chem. Soc.* **2011**, *133* (25), 9638–9641. <https://doi.org/10.1021/ja201131h>.
- (49) Liang, Y.; Feng, D.; Wu, Y.; Tsai, S.-T.; Li, G.; Ray, C.; Yu, L. Highly Efficient Solar Cell Polymers Developed via Fine-Tuning of Structural and Electronic Properties. *J. Am. Chem. Soc.* **2009**, *131* (22), 7792–7799. <https://doi.org/10.1021/ja901545q>.
- (50) Szarko, J. M.; Guo, J.; Liang, Y.; Lee, B.; Rolczynski, B. S.; Strzalka, J.; Xu, T.; Loser, S.; Marks, T. J.; Yu, L.; et al. When Function Follows Form: Effects of Donor Copolymer Side Chains on Film Morphology and BHJ Solar Cell Performance. *Adv. Mater.* **2010**, *22* (48), 5468–5472. <https://doi.org/10.1002/adma.201002687>.
- (51) van Mullekom, H. A. M.; Vekemans, J. A. J. M.; Havinga, E. E.; Meijer, E. W. Developments in the Chemistry and Band Gap Engineering of Donor–Acceptor Substituted Conjugated Polymers. *Mater. Sci. Eng. R Rep.* **2001**, *32* (1), 1–40. [https://doi.org/10.1016/S0927-796X\(00\)00029-2](https://doi.org/10.1016/S0927-796X(00)00029-2).
- (52) Bundgaard, E.; Krebs, F. C. Low Band Gap Polymers for Organic Photovoltaics. *Sol. Energy Mater. Sol. Cells* **2007**, *91* (11), 954–985. <https://doi.org/10.1016/j.solmat.2007.01.015>.
- (53) Chochos, C. L.; Choulis, S. A. How the Structural Deviations on the Backbone of Conjugated Polymers Influence Their Optoelectronic Properties and Photovoltaic Performance. *Progress in Polymer Science* **2011**, *36* (10), 1326–1414. <https://doi.org/10.1016/j.progpolymsci.2011.04.003>.
- (54) Meng, L.; Zhang, Y.; Wan, X.; Li, C.; Zhang, X.; Wang, Y.; Ke, X.; Xiao, Z.; Ding, L.; Xia, R.; et al. Organic and Solution-Processed Tandem Solar Cells with 17.3% Efficiency. *Science* **2018**, *361* (6407), 1094–1098. <https://doi.org/10.1126/science.aat2612>.
- (55) Climate information for solar energy <http://www.bom.gov.au/climate/data-services/solar/#tabs=Understanding> (accessed Jan 21, 2019).
- (56) Solar Spectra | Grid Modernization | NREL <https://www.nrel.gov/grid/solar-resource/spectra.html> (accessed Jan 21, 2019).
- (57) Standard Solar Spectra | PVEducation <https://www.pveducation.org/pvcdrom/appendices/standard-solar-spectra> (accessed Jan 21, 2019).
- (58) Gueymard, C. A.; Myers, D.; Emery, K. Proposed Reference Irradiance Spectra for Solar Energy Systems Testing. *Sol. Energy* **2002**, *73* (6), 443–467. [https://doi.org/10.1016/S0038-092X\(03\)00005-7](https://doi.org/10.1016/S0038-092X(03)00005-7).
- (59) Thomsen, E. A. Characterisation of Materials for Organic Photovoltaics. Thesis, University of St Andrews: United Kingdom, 2008.
- (60) Woods, K. W. Solar Energy Conversion and Control Using Organic Photovoltaic Cells. Thesis, Western Kentucky University: Kentucky, USA, 2013.
- (61) California Scientific Inc. Solar Cell Characterization <http://www.californiascientific.com/resource.htm> (accessed Jan 21, 2019).

- (62) Waldauf, C.; Scharber, M. C.; Schilinsky, P.; Hauch, J. A.; Brabec, C. J. Physics of Organic Bulk Heterojunction Devices for Photovoltaic Applications. *J. Appl. Phys.* **2006**, *99* (10), 104503. <https://doi.org/10.1063/1.2198930>.
- (63) Brabec, C. J.; Shaheen, S. E.; Winder, C.; Sariciftci, N. S.; Denk, P. Effect of LiF/Metal Electrodes on the Performance of Plastic Solar Cells. *Appl. Phys. Lett.* **2002**, *80* (7), 1288–1290. <https://doi.org/10.1063/1.1446988>.
- (64) Adhikary, P.; Venkatesan, S.; Adhikari, N.; Maharjan, P. P.; Adebajo, O.; Chen, J.; Qiao, Q. Enhanced Charge Transport and Photovoltaic Performance of PBDTTT-C-T/PC70BM Solar Cells via UV–Ozone Treatment. *Nanoscale* **2013**, *5* (20), 10007–10013. <https://doi.org/10.1039/C3NR03355D>.
- (65) Zhou, Y.; Fuentes-Hernandez, C.; Shim, J.; Meyer, J.; Giordano, A. J.; Li, H.; Winget, P.; Papadopoulos, T.; Cheun, H.; Kim, J.; et al. A Universal Method to Produce Low–Work Function Electrodes for Organic Electronics. *Science* **2012**, *336* (6079), 327–332. <https://doi.org/10.1126/science.1218829>.
- (66) Sista, S.; Hong, Z.; Chen, L.-M.; Yang, Y. Tandem Polymer Photovoltaic Cells—Current Status, Challenges and Future Outlook. *Energy Environ. Sci.* **2011**, *4* (5), 1606–1620. <https://doi.org/10.1039/C0EE00754D>.
- (67) You, J.; Dou, L.; Yoshimura, K.; Kato, T.; Ohya, K.; Moriarty, T.; Emery, K.; Chen, C.-C.; Gao, J.; Li, G.; et al. A Polymer Tandem Solar Cell with 10.6% Power Conversion Efficiency. *Nat. Commun.* **2013**, *4*, 1446. <https://doi.org/10.1038/ncomms2411>.
- (68) Etxebarria, I.; Ajuria, J.; Pacios, R. Solution-Processable Polymeric Solar Cells: A Review on Materials, Strategies and Cell Architectures to Overcome 10%. *Org. Electron.* **2015**, *19*, 34–60. <https://doi.org/10.1016/j.orgel.2015.01.014>.
- (69) How a Solar Cell Works  
<https://www.acs.org/content/acs/en/education/resources/highschool/chemmatters/past-issues/archive-2013-2014/how-a-solar-cell-works.html> (accessed Jan 23, 2019).
- (70) Bagher, A. M. Comparison of Organic Solar Cells and Inorganic Solar Cells. *Int. J. Sustain. Green Energy* **2014**, *3* (3), 53. <https://doi.org/10.11648/j.ijrse.20140303.12>.
- (71) Bogdal, D. Chapter 1 - Interaction of Microwaves with Different Materials. In *Tetrahedron Organic Chemistry Series*; Bogdal, D., Ed.; Microwave-assisted Organic Synthesis; Elsevier, 2005; Vol. 25, pp 1–11. [https://doi.org/10.1016/S1460-1567\(05\)80014-5](https://doi.org/10.1016/S1460-1567(05)80014-5).
- (72) Gregg, B. A.; Hanna, M. C. Comparing Organic to Inorganic Photovoltaic Cells: Theory, Experiment, and Simulation. *J. Appl. Phys.* **2003**, *93* (6), 3605–3614. <https://doi.org/10.1063/1.1544413>.
- (73) Berger, P. R.; Kim, M. Polymer Solar Cells: P3HT:PCBM and Beyond. *J. Renew. Sustain. Energy* **2018**, *10* (1), 013508. <https://doi.org/10.1063/1.5012992>.
- (74) Mikhnenko, O. V.; Blom, P. W. M.; Nguyen, T.-Q. Exciton Diffusion in Organic Semiconductors. *Energy Environ. Sci.* **2015**, *8* (7), 1867–1888. <https://doi.org/10.1039/C5EE00925A>.

- (75) Hiramoto, M.; Kubo, M.; Shinmura, Y.; Ishiyama, N.; Kaji, T.; Sakai, K.; Ohno, T.; Izaki, M. Bandgap Science for Organic Solar Cells. *Electronics* **2014**, *3* (2), 351–380. <https://doi.org/10.3390/electronics3020351>.
- (76) Scholes, G. D. Long-Range Resonance Energy Transfer in Molecular Systems. *Annu. Rev. Phys. Chem.* **2003**, *54*, 57–87. <https://doi.org/10.1146/annurev.physchem.54.011002.103746>.
- (77) Dexter, D. L. A Theory of Sensitized Luminescence in Solids. *J. Chem. Phys.* **1953**, *21* (5), 836–850. <https://doi.org/10.1063/1.1699044>.
- (78) Band gap - Energy Education [https://energyeducation.ca/encyclopedia/Band\\_gap#cite\\_note-RE2-1](https://energyeducation.ca/encyclopedia/Band_gap#cite_note-RE2-1) (accessed Jan 24, 2019).
- (79) Rwenyagila, E. R. A Review of Organic Photovoltaic Energy Source and Its Technological Designs. *Int. J. Photoenergy* **2017**, *2017*, 12. <https://doi.org/10.1155/2017/1656512>.
- (80) Kroon, R.; Lenes, M.; Hummelen, J. C.; Blom, P. W. M.; Boer, B. de. Small Bandgap Polymers for Organic Solar Cells (Polymer Material Development in the Last 5 Years). *Polym. Rev.* **2008**, *48* (3), 531–582. <https://doi.org/10.1080/15583720802231833>.
- (81) Hess, B. Andes.; Schaad, L. J. Hueckel Molecular Orbital .Pi.-Resonance Energies. Heterocycles Containing Divalent Sulfur. *J. Am. Chem. Soc.* **1973**, *95* (12), 3907–3912. <https://doi.org/10.1021/ja00793a013>.
- (82) Hess, B. A.; Schaad, L. J.; Holyoke, C. W. On the Aromaticity of Heterocycles Containing the Amine Nitrogen or the Ether Oxygen. *Tetrahedron* **1972**, *28* (14), 3657–3667. [https://doi.org/10.1016/S0040-4020\(01\)93812-8](https://doi.org/10.1016/S0040-4020(01)93812-8).
- (83) Varshni, Y. P. Temperature Dependence of the Energy Gap in Semiconductors. *Physica* **1967**, *34* (1), 149–154. [https://doi.org/10.1016/0031-8914\(67\)90062-6](https://doi.org/10.1016/0031-8914(67)90062-6).
- (84) DoITPoMS - TLP Library Introduction to Semiconductors - Direct and Indirect Band Gap Semiconductors <https://www.doitpoms.ac.uk/tlplib/semiconductors/direct.php> (accessed Jan 31, 2019).
- (85) Yuan, L.-D.; Deng, H.-X.; Li, S.-S.; Luo, J.-W.; Wei, S.-H. Unified Theory of the Direct or Indirect Bandgap Nature of Conventional Semiconductors. *Phys. Rev. B* **2018**, *98* (24). <https://doi.org/10.1103/PhysRevB.98.245203>.
- (86) Simon, S. H. *The Oxford Solid State Basics*; OUP Oxford, 2013.
- (87) Tauc, J.; Menth, A. States in the Gap. *J. Non-Cryst. Solids* **1972**, *8–10*, 569–585. [https://doi.org/10.1016/0022-3093\(72\)90194-9](https://doi.org/10.1016/0022-3093(72)90194-9).
- (88) Davis, E. A.; Mott, N. F. Conduction in Non-Crystalline Systems V. Conductivity, Optical Absorption and Photoconductivity in Amorphous Semiconductors. *Philos. Mag. J. Theor. Exp. Appl. Phys.* **1970**, *22* (179), 0903–0922. <https://doi.org/10.1080/14786437008221061>.
- (89) Xu, T.; Yu, L. How to Design Low Bandgap Polymers for Highly Efficient Organic Solar Cells. *Mater. Today* **2014**, *17* (1), 11–15. <https://doi.org/10.1016/j.mattod.2013.12.005>.

- (90) Nunzi, J.-M. Organic Photovoltaic Materials and Devices. *Comptes Rendus Phys.* **2002**, *3* (4), 523–542. [https://doi.org/10.1016/S1631-0705\(02\)01335-X](https://doi.org/10.1016/S1631-0705(02)01335-X).
- (91) Polman, A.; Atwater, H. A. Photonic Design Principles for Ultrahigh-Efficiency Photovoltaics. *Nat. Mater.* **2012**, *11*, 174–177. <https://doi.org/10.1038/nmat3263>.
- (92) Landsberg, P. T.; Tonge, G. Thermodynamic Energy Conversion Efficiencies. *J. Appl. Phys.* **1980**, *51* (7), R1–R20. <https://doi.org/10.1063/1.328187>.
- (93) Green, M. A.; Emery, K.; Hishikawa, W.; Warta, W.; Dunlop, E. D. Solar Cell Efficiency Tables (Version 39). *Progress in Photovoltaics, Research and Applications* **2012**, *20* (1), 12–20.
- (94) Lunt, R. R.; Osedach, T. P.; Brown, P. R.; Rowehl, J. A.; Bulović, V. Practical Roadmap and Limits to Nanostructured Photovoltaics. *Adv. Mater.* **2011**, *23* (48), 5712–5727. <https://doi.org/10.1002/adma.201103404>.
- (95) Levy, M. Y.; Honsberg, C. Rapid and Precise Calculations of Energy and Particle Flux for Detailed-Balance Photovoltaic Applications. *Solid-State Electron.* **2006**, *50* (7), 1400–1405. <https://doi.org/10.1016/j.sse.2006.06.017>.
- (96) Koster, L. J. A.; Mihailetschi, V. D.; Bloom, P. W. M. The Optimal Band Gap for Plastic Photovoltaics. *SPIE News Room* **2007**, 9–10. <https://doi.org/10.1117/2.1200701.0528>.
- (97) Short-Circuit Current | PVEducation <https://www.pveducation.org/pvcdrom/solar-cell-operation/short-circuit-current> (accessed Jan 28, 2019).
- (98) Koster, L. J. A.; Mihailetschi, V. D.; Blom, P. W. M. Ultimate Efficiency of Polymer/Fullerene Bulk Heterojunction Solar Cells. *Appl. Phys. Lett.* **2006**, *88* (9), 093511. <https://doi.org/10.1063/1.2181635>.
- (99) SpectroVis® Plus Spectrophotometer | Vernier <https://www.vernier.com/products/sensors/spectrometers/visible-range/svis-pl/#section4> (accessed Jan 31, 2019).
- (100) Hrostea, L.; Girtan, M.; Mallet, R.; Leontie, L. Optical and Morphological Properties of P3HT and P3HT:PCBM Thin Films Used in Photovoltaic Applications. **2018**, *374*. <https://doi.org/10.1088/1757-899X/374/1/012015>.
- (101) Kwon, O.; McKee, M. L. Calculations of Band Gaps in Polyaniline from Theoretical Studies of Oligomers. *J. Phys. Chem. B* **2000**, *104* (8), 1686–1694. <https://doi.org/10.1021/jp9910946>.
- (102) Mishra, R.; Tripathy, S. P.; Sinha, D.; Dwivedi, K. K.; Ghosh, S.; Khathing, D. T.; Chung, W. H. Optical and Electrical Properties of Some Electron and Proton Irradiated Polymers. *Nuclear Instruments and Methods in Physics Research Section B: Beam Interactions with Materials and Atoms* **2000**, *168* (1), 59–64. [https://doi.org/10.1016/S0168-583X\(99\)00829-0](https://doi.org/10.1016/S0168-583X(99)00829-0).
- (103) Shockley, W.; Queisser, H. J. Detailed Balance Limit of Efficiency of P-n Junction Solar Cells. *J. Appl. Phys.* **1961**, *32*, 510–519. <https://doi.org/10.1063/1.1736034>.
- (104) Drobny, J. Properties of Styrene-Isobutylene-Styrene Block Copolymers. In *Specialty Thermoplastics*; Drobny, J., Ed.; Landolt-Börnstein - Group VIII

- Advanced Materials and Technologies; Springer Berlin Heidelberg: Berlin, Heidelberg, 2015; pp 148–150. [https://doi.org/10.1007/978-3-662-46419-9\\_39](https://doi.org/10.1007/978-3-662-46419-9_39).
- (105) Anani, M.; Mathieu, C.; Lebid, S.; Amar, Y.; Chama, Z.; Abid, H. Model for Calculating the Refractive Index of a III–V Semiconductor. *Comput. Mater. Sci.* **2008**, *41* (4), 570–575. <https://doi.org/10.1016/j.commatsci.2007.05.023>.
- (106) Jung, S. D.; Hwang, W. Y.; Song, S. H.; Lee, el-H.; Lee, J. I.; Shim, H. K. Sulfonated Polystyrene as a New Gradient-Index Medium for Light-Focusing Elements. *Opt. Lett.* **1995**, *20* (11), 1236–1237.
- (107) Liao, Y.; Strong, V.; Chian, W.; Wang, X.; Li, X.-G.; Kaner, R. B. Sulfonated Polyaniline Nanostructures Synthesized via Rapid Initiated Copolymerization with Controllable Morphology, Size, and Electrical Properties. *Macromolecules* **2012**, *45* (3), 1570–1579. <https://doi.org/10.1021/ma2024446>.
- (108) Phiri, J.; Johansson, L.-S.; Gane, P.; Maloney, T. A Comparative Study of Mechanical, Thermal and Electrical Properties of Graphene-, Graphene Oxide- and Reduced Graphene Oxide-Doped Microfibrillated Cellulose Nanocomposites. *Compos. Part B Eng.* **2018**, *147*, 104–113. <https://doi.org/10.1016/j.compositesb.2018.04.018>.
- (109) Wang, Z.; Li, P.; Chen, Y.; He, J.; Zhang, W.; Schmidt, O. G.; Li, Y. Pure Thiophene–Sulfur Doped Reduced Graphene Oxide: Synthesis, Structure, and Electrical Properties. *Nanoscale* **2014**, *6* (13), 7281–7287. <https://doi.org/10.1039/C3NR05061K>.
- (110) Poly(ether ether ketone)  
<http://polymerdatabase.com/polymers/polyetheretherketone.html> (accessed Feb 11, 2019).
- (111) Brodkorb, F.; Fischer, B.; Kalbfleisch, K.; Robers, O.; Braun, C.; Dohlen, S.; Kreyenschmidt, J.; Lorenz, R.; Kreyenschmidt, M. Development of a New Monomer for the Synthesis of Intrinsic Antimicrobial Polymers with Enhanced Material Properties. *Int. J. Mol. Sci.* **2015**, *16* (8), 20050–20066. <https://doi.org/10.3390/ijms160820050>.
- (112) 2-(tert-Butylamino)ethyl methacrylate, min. 90%  
<http://www.polysciences.com/default/catalog-products/2-tert-butylaminoethyl-methacrylate-min-90> (accessed Apr 22, 2019).
- (113) Aziz, S. B.; Hussein, S.; Hussein, A. M.; Saeed, S. R. Optical Characteristics of Polystyrene Based Solid Polymer Composites: Effect of Metallic Copper Powder <https://www.hindawi.com/journals/ijmet/2013/123657/> (accessed Feb 15, 2019). <https://doi.org/10.1155/2013/123657>.
- (114) Polystyrene | Sigma-Aldrich  
<https://www.sigmaaldrich.com/catalog/substance/polystyrene12345900353611?lang=en&region=US&attrlist=Refractive%20Index> (accessed Feb 15, 2019).
- (115) Haq, K.; Shan-peng, L.; Khan, M. A.; Jiang, X. Y.; Zhang, Z. L.; Zhu, W. Q. Red Organic Light-Emitting Diodes Based on Wide Band Gap Emitting Material as the Host Utilizing Two-Step Energy Transfer. *Semicond. Sci. Technol.* **2008**, *23* (3), 035024. <https://doi.org/10.1088/0268-1242/23/3/035024>.

- (116) Gao, C.; Zhang, S.; Lin, Y.; Li, F.; Guan, S.; Jiang, Z. High-Performance Conductive Materials Based on the Selective Location of Carbon Black in Poly(Ether Ether Ketone)/Polyimide Matrix. *Compos. Part B Eng.* **2015**, *79*, 124–131. <https://doi.org/10.1016/j.compositesb.2015.03.047>.
- (117) Yang, L.; Zhang, S.; Chen, Z.; Guo, Y.; Luan, J.; Geng, Z.; Wang, G. Design and Preparation of Graphene/Poly(Ether Ether Ketone) Composites with Excellent Electrical Conductivity. *J. Mater. Sci.* **2014**, *49* (5), 2372–2382. <https://doi.org/10.1007/s10853-013-7940-2>.
- (118) Poly(ethylene glycol) methyl ether methacrylate 447943  
<https://www.sigmaaldrich.com/catalog/product/aldrich/447943> (accessed Feb 20, 2019).
- (119) Rumer, J. W.; McCulloch, I. Organic Photovoltaics: Crosslinking for Optimal Morphology and Stability. *Mater. Today* **2015**, *18* (8), 425–435. <https://doi.org/10.1016/j.mattod.2015.04.001>.

## 7 APPENDIX

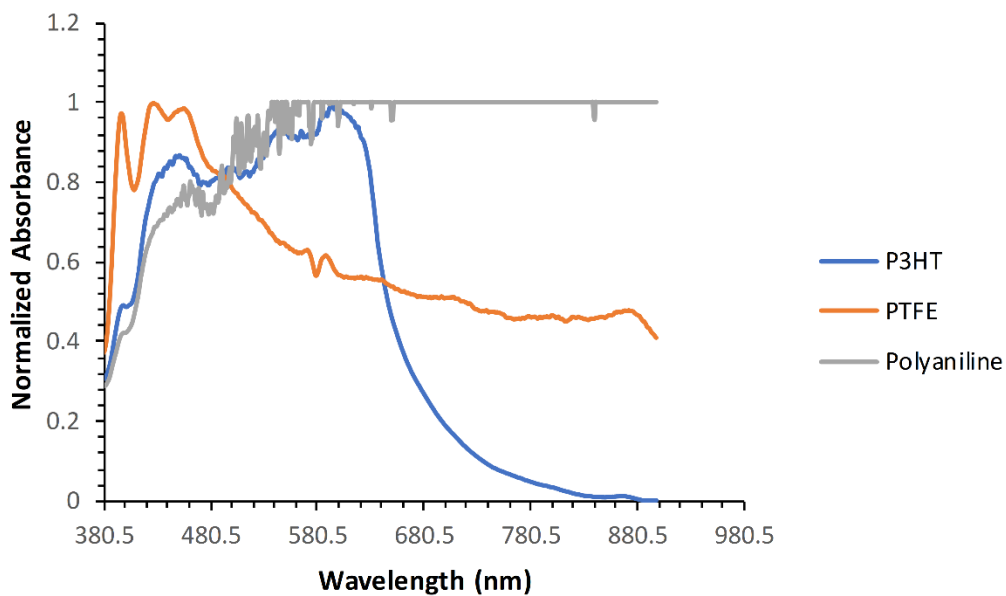


Figure 7.1-Normalized absorbance for P3HT, PTFE and Polyaniline.

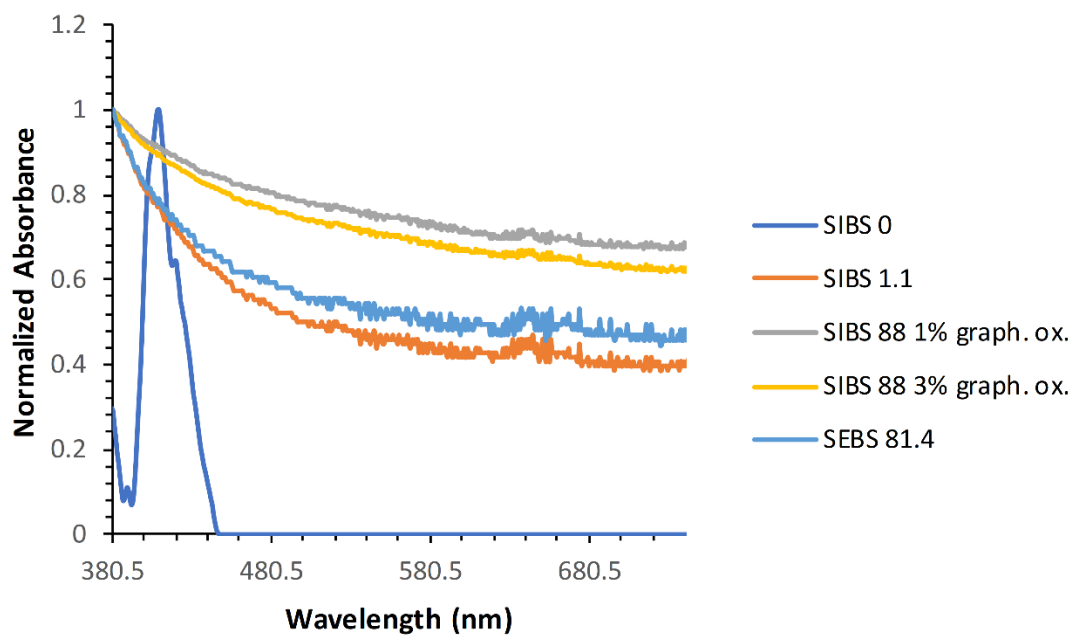


Figure 7.2-Normalized absorbance for SIBS and SEBS polymers.

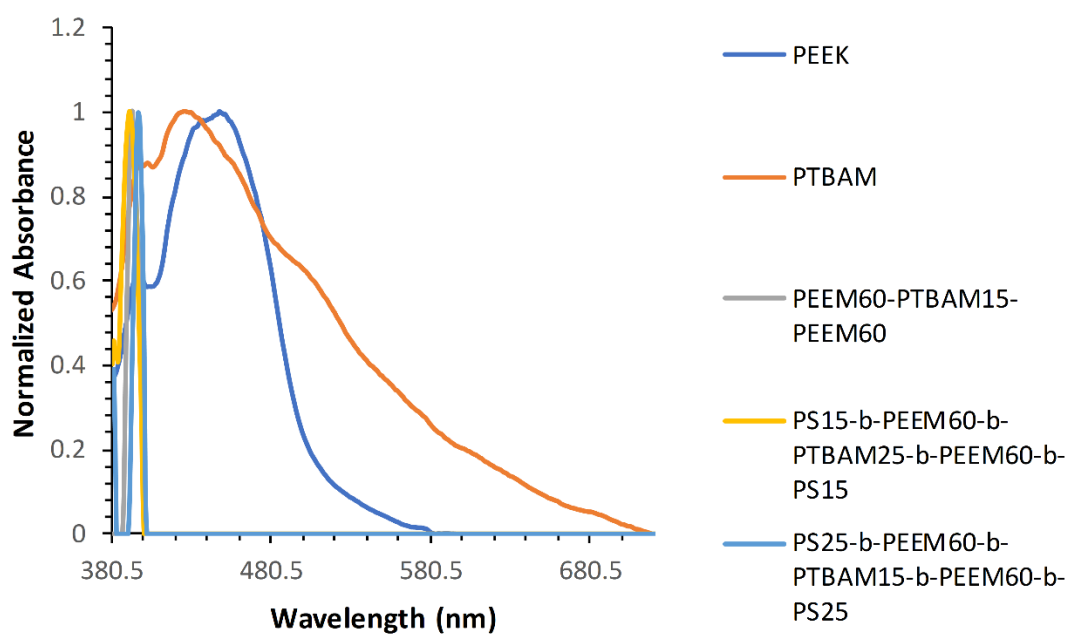


Figure 7.3-Normalized absorbance for PEEK, PTBAM and block polymers.

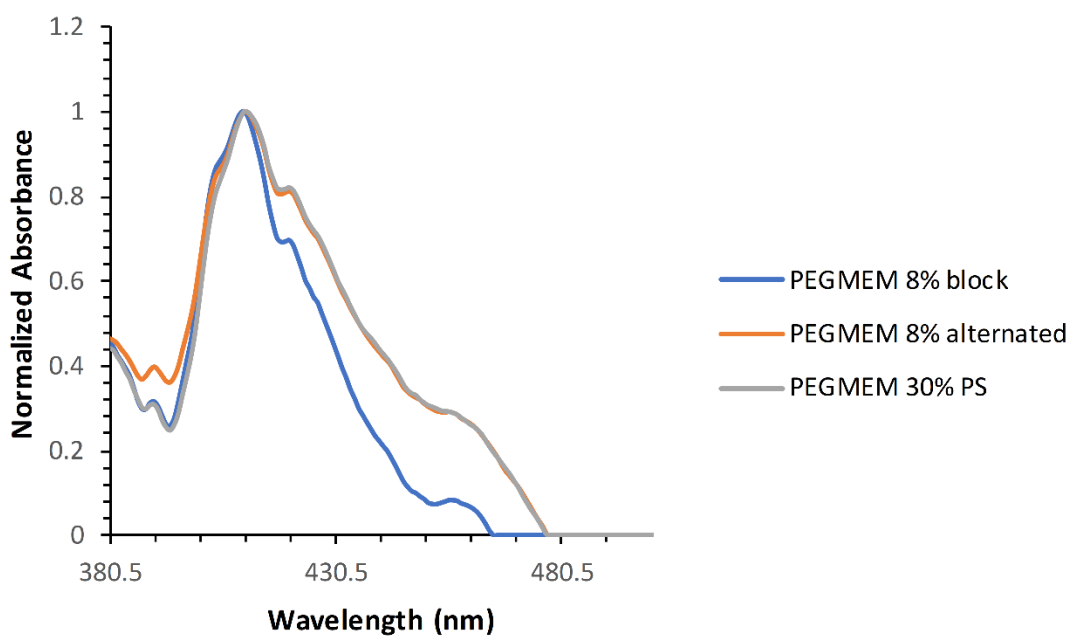


Figure 7.4-Normalized absorbance for EGMEM polymers.